AD

AD-E400 954

TECHNICAL REPORT ARPAD-TR-81007

INCREASING THE CLARITY OF ULTRASONIC CRACK DETECTION SIGNALS FROM BASES MOUNTED ONTO LOADED 155-MM M483A1 PROJECTILES

HENRY HARTMANN

JANUARY 1983

US ARMY ARMAMENT RESEARCH AND DEVELOPMENT COMMAND
PRODUCT ASSURANCE DIRECTORATE
DOVER, NEW JERSEY

UNCLASSIFIED

SECURITY CLASSIFICATION OF THIS PAGE *(When Data Entered)*

REPORT DOCUMENTATION PAGE		READ INSTRUCTIONS BEFORE COMPLETING FORM
1. REPORT NUMBER Technical Report ARPAD-TR-81007	2. GOVT ACCESSION NO.	3. RECIPIENT'S CATALOG NUMBER
4. TITLE *(and Subtitle)* INCREASING THE CLARITY OF ULTRASONIC CRACK DETECTION SIGNALS FROM BASES MOUNTED ONTO LOADED 155-mm M483A1 PROJECTILES		5. TYPE OF REPORT & PERIOD COVERED Final Sep 1981 6. PERFORMING ORG. REPORT NUMBER
7. AUTHOR(s) Henry Hartmann		8. CONTRACT OR GRANT NUMBER(s)
9. PERFORMING ORGANIZATION NAME AND ADDRESS ARRADCOM, PAD Technology & Automation, Information & Mathematics Div (DRDAR-QAS-T) Dover, NJ 07801		10. PROGRAM ELEMENT, PROJECT, TASK AREA & WORK UNIT NUMBERS
11. CONTROLLING OFFICE NAME AND ADDRESS ARRADCOM, TSD STINFO Div (DRDAR-TSS) Dover, NJ 07801		12. REPORT DATE January 1983 13. NUMBER OF PAGES 54
14. MONITORING AGENCY NAME & ADDRESS*(if different from Controlling Office)*		15. SECURITY CLASS. *(of this report)* Unclassified 15a. DECLASSIFICATION/DOWNGRADING SCHEDULE

16. DISTRIBUTION STATEMENT *(of this Report)*

Approved for public release; distribution unlimited.

17. DISTRIBUTION STATEMENT *(of the abstract entered in Block 20, if different from Report)*

18. SUPPLEMENTARY NOTES

19. KEY WORDS *(Continue on reverse side if necessary and identify by block number)*

Adapters
Artillery ammunition
Base
Cracks
Projectiles
Ultrasonic test

20. ABSTRACT *(Continue on reverse side if necessary and identify by block number)*

Ultrasonic inspection of bases on loaded 155-mm M483A1 projectiles can be hampered by adapter signals caused by contact between base, shim, and adapters. The presence of adapter signals tends to mask the detection signal from cracks. This report offers several ways for enhancing ultrasonic detection signals from cracks in bases fastened to loaded projectiles.

DD FORM 1 JAN 73 1473 EDITION OF 1 NOV 65 IS OBSOLETE

UNCLASSIFIED

SECURITY CLASSIFICATION OF THIS PAGE *(When Data Entered)*

CONTENTS

TABLES

FIGURES

INTRODUCTION

Cracked bases have been found on loaded 155-mm M483A1 projectiles (fig. 1). A nondestructive inspection technique is needed to screen the involved portion of stockpile. Ultrasonic inspection provides the best capablity for inspecting bases that are still attached to loaded projectiles.

Initial ultrasonic inspection revealed unexpected reflection signals (called "adapter signals") coming from the forward surface of the base. These signals occurred where the adapters firmly pressed a shim against the forward surface of the base (fig. 2). These reflection signals can mask the presence of cracks (fig. 3). Reduction of amplitude of adapter signals relative to crack signals is needed for reliable ultrasonic inspection.

Seven ultrasonic inspection parameters were investigated for their impact upon the ultrasonic echo signals. In addition, the advantage of the use of dual, offset, ultrasonic inspection transducers is displayed.

METHOD OF ATTACK

The following parameters were investigated to determine their influence on crack signals versus adapter signals.

1. Angle-of-refraction of shear wave
2. Frequency of transducer
3. Filtering of echo signal
4. Tuning of receiver signal
5. Frequency bandwidth of ultrasound pulse
6. Focusing of ultrasound pulse
7. Direction of ultrasound pulse

INVESTIGATION

General

Ultrasonic laboratory scanners at ARRADCOM are not deep enough to accept a full-sized M483A1 projectile standing on its nose. Therefore, only the rear portion of a projectile body was used. This assembly was made by cutting off the rear of a projectile body and welding it to a plate. The plate provided a means for retaining the contents as well as sealing the assembly. Inert grenades,

adapters, and shims were loaded into this assembly; and base CMC/KAAP 54 (containing a known crack) was tightened down to the proper torque (fig. 4). The resulting simulated projectile easily fit into the tank of the laboratory scanner.

The simulated projectile was centered on the turntable of the laboratory scanner. Water was placed inside the rear cavity of the base to act as a coupling. Ultrasonic data were recorded from both adapter signals and crack signals under many different conditions.

Four locations on the base were selected for monitoring. Two of these locations were where the adapter signals were most intense; the other two were where the crack signals were greatest. (The distribution of adapter signals is called "pressure patterns.") For the various conditions imposed, peak ultrasonic signals were recorded from these four locations. Several of the parameters were evaluated, one at a time, and data were recorded (table 1).

For each condition, an ultrasonic C-scan was made of the cracked base (which was part of the simulated projectile). The four prominent locations were identified on each C-scan, and their signal strengths were recorded. That is, the gain setting of the flaw detector was recorded when each signal was 50% of screen height. Thus, stronger signals have lower gain setting readings.

An S-80 Reflectoscope ultrasonic flaw detector was used, together with a UI-450 Laboratory Scanner. The water tank was kept dry.

Parameters

Angle-of-Refraction of Shear Wave

Prior work had revealed that optimum sensitivity of detection and clarity of detection were produced by a 39 degree angle-of-refraction shear wave. These optimum sensitivities had been achieved with a 5.0 MHz, 6.4 mm (0.25 in.) diameter, flat lensed transducer. Since other transducers (both focused and unfocused) were to be investigated, refraction angles ranging from approximately 35 to 55 degrees were tried.

Frequency of Transducer

A peak frequency of 5 MHz is popular for the ultrasonic inspection of aluminum. In this investigation, both 5 MHz and 10 MHz peak frequencies were evaluated.

Filtering of Echo Signal

The S-80 Reflectoscope permits the filtering out of high frequency components from the received echo signal. The filter switch has four settings--off, 1, 2, and 3. The higher the numbered setting, the greater the filtering of the echo signal.

Tuning of Receiver Signal

The S-80 Reflectoscope permits tuning of its receiver for specific frequencies of interest; that is, the echo signal is filtered above and below the spectrum of interest. In addition, no tuning can be selected by setting the control switch on WB (wideband). For this investigation, 5-MHz transducers were evaluated at a tuned setting of 5 MHz and at an untuned setting of WB. Ten-MHz transducers were likewise evaluated at 10 MHz and at WB settings.

Frequency Bandwidth of Ultrasound Pulse

The transducer determines the bandwidth of the pulsed ultrasound signal. Highly damped transducers emit wideband pulses of ultrasound. Relatively undamped transducers emit narrowband pulses. Three narrowband and one wideband frequency transducers were used. Two transducers of each narrow and wide bandwidth would have been preferred but what was available had to be used.

Focusing of Ultrasound Pulse

A far field of ultrasound naturally focuses at a certain distance from an emitting transducer. A lens on a transducer can bring the focal zone closer and make it more intense. In this investigation, both focused (spherical lens) and nonfocused (flat lens) transducers were used. Focal distances were 102 mm (4 in.).

Gain

The minimum gain needed to detect the crack at 50% height-of-screen is listed for each transducer in table 2.

Direction of Ultrasound Pulse

Most of the data were obtained from ultrasound pulsed radially through the cracked base. Near the end of the investigation, the possibility of using

dual transducers was considered. Therefore, some data were obtained by offsetting a transducer from the center of the cracked base. In effect, this offset gave the ultrasound pulses a slight circumferential component of movement.

ANALYSIS

General

Most of the data in table 1 are plotted in figures 5 through 8. Some data where signal-to-noise ratios are low, such as highly filtered signals, were not included in these figures.

The word "clarity" normally refers to a signal-to-noise ratio. That is, a clear signal is one where very little or no noise exists. In this anaysis, "noise" refers to adapter signals, since these signals are undesirable. Therefore, the plots show the ratio of crack detection signals to adapter detection signals.

The depth of the crack in the base was measured by use of 39 degree angle-of-refraction shear waves. A standard containing seven round-bottomed holes was used to calibrate the echo signals on the cathode-ray-tube screen of the flaw detector. The accuracy of calibration was within 0.5 mm (0.02 in.). The deepest section of crack was 1.0 mm (0.04 in.).

The best performance (greatest clarity) was demonstrated by transducers A and B (table 2; figs. 5 and 6). Both of these ultrasonic transducers achieved clarities of 17 decibels; that is, the ratio of crack detection signal to adapter detection signal is 7.1:1. Close behind, with a peak clarity of 16 decibels (crack-signal-to-adapter-signal ratio 6.3:1), was transducer C (fig. 7). Finally, with a peak performance of 15 decibels (crack-signal-to-adapter-signal ratio of 5.6:1), was transducer D (fig. 8).

Parameters

Angle-of-Refraction of Shear Waves

One of the top performances was accomplished by transducer A (fig. 5). Transducer A was quite selective in its shear wave angle-of-refraction. Peak performance occurred at a refracted angle-of-shear of 41 degrees.

An even better shear wave angle-of-refraction was evident in the performance of transducer B (fig. 6). The peak performance occurred at a refracted angle-of-shear between 39 and 41 degrees.

The other two transducers provided a more uniform level of performance over the complete range of angle-of-refraction of shear waves.

Frequency of Transducer

No relationship was established between frequency and clarity. (However, the lower frequency of 5 MHz peak produced stronger crack echoes.)

Filtering of Echo Signal

Slight filtering at setting f1 provided the means by which transducer B produced its best performance. None of the other transducers needed any filtering for peak performance. (The addition of filtering caused a need for more gain.)

Tuning of Receiver Signal

Three of the four transducers, including the two with top performance, depended upon tuned receiver signals for greatest clarity of crack detection signals.

Frequency Bandwidth of Ultrasound Pulse

Insufficient evidence exists to determine the influence of highly damped versus relatively undamped transducers on the clarity of crack detection signals. One of the top performing transducers had a wideband pulse, whereas the other three transducers had narrowband pulses.

Focusing of Ultrasound Pulse

Evidence fails to pinpoint the merits of focused pulses of ultrasound. One of the two top performing transducers was focused, whereas the other one was not.

Direction of Ultrasound Pulse

Cracks in bases are rough surfaced separations that do not exactly follow circumferential orientations. Therefore, two transducers aimed at the same location of a crack and slightly to the left and right of a radial position, can obtain echo signals which, when superimposed, should be more descriptive of the presence of a crack than signals from only one transducer. At the same time, since neither of the two transducers is aimed normal to the machining ridges on the forward suface of the base, superimposed signals from the adapters (noise) should be less than one normally aimed signal.

C-scans were made from varying offsets, both left and right. The angle away from a radial position (α) varied inversely with the distance of the inspection zone away from the center of the base (fig. 9). That is, out near the rim of the base, a slight offset of the transducer would cause only a small change in the angular setting away from a radial position. However, as the ultrasonic inspection region approached the center of the base, the angle from a radial position increased until it finally reached 90 degrees. Any offset from a radial inspection position causes a circumferential inspection to occur in the base at the distance equal to that of the offset out from the center of the base.

Using figure 10 as a reference, when an additional offset of the transducer of only 1 mm (0.04 in.) was induced and another C-scan recorded (fig. 11), adapter signals decreased rapidly. The greatest reduction occurred toward the center of the base where the strongest signal (5 db on the center adapter) disappeared. Further out towards the perimeter, a portion of only a 1-decibel adapter signal still remains. This occurrence reveals that the inspection orientation with the metal machining ridges on the forward surface of the base affect the intensity of the adapter signals. If these tiny machined ridges were not present, chances are that ultrasonic signals from the pressure of the adapters would not be a problem. Since the orientation of most deep cracks is circumferential, a radial crack detection position of a transducer (which will be normal to these cracks) is the best orientation.

More ultrasonic C-scans at other distances of offset were produced (figs. 12 through 21).

Transparencies were made of each offset-transducer C-scan and these were superimposed for matching offset distances. The results reveal reductions in both adapter and crack signals. As expected, the superimposed echo signals (figs. 22 through 27) maintain the size of the crack image much better than they maintain the image of the adapters.

CONCLUSIONS

1. The ultrasonic echo noise from unwanted adapter signals is greatest when pulsed in a radial direction.

2. Radially oriented ultrasonic inspection with sensitivity to reveal 1 mm deep cracks will also reveal adapter signals.

3. A 41 degree angle-of-refraction of shear waves was most popular (three out of four) for maximum clarity (crack detection signal/adapter detection signal).

4. Tuning the receiver enhanced the clarity of three out of four transducers.

5. The 5 MHz focused ultrasonic transducer needed at least 30 db less gain than the other transducers.

6. Slight filtering enhanced the clarity of one out of four transducers.

7. Transducer bandwidths, focusing, and frequency parameters did not demonstrate significant improvements in clarity.

8. Superimposing ultrasonic flaw detection signals from dual transducers which are slightly angled (in order to inspect the same spot) can preserve crack signals while diminishing adapter signals.

RECOMMENDATIONS

It is recommended that at least 12 cracked bases be selected for further investigation. These bases should include cracks of various depths and locations. The amplitude of the crack detection signal should be compared to that of the maximum adapter signal. Features already proven desirable should be used in the future work. As part of this future investigation, the advantages of offsetting a transducer should be evaluated further.

Table 1. Ultrasonic test data for a cracked base mounted in a simulated projectile body

Transducer angle-of-incidence (deg)	Settings on S-80 Reflectoscope					
			Gain for 50% screen height of signal (db)			
			Adapter		Crack	
	Frequency (MHz)	Filter	For point 1	For point 2	For point 1	For point 2
			TRANSDUCER A[a]			
16	5		14	17	1	12
		1	21	24	7	19
		2	23	27	10	22
		3	27	31	15	27
	WB		23	25	13	23
		1	29	31	17	30
		2	32	35	21	33
		3	37	39	27	39
17.3	5		15	20	5	15
		1	21	26	11	21
		2	24	28	14	25
		3	28	33	20	29
	WB		24	27	14	26
		1	30	33	21	32
		2	33	36	25	35
		3	38	41	31	41

[a] Peak frequency 5 MHz, narrowband, 19 mm (0.75 in.) active element diameter, cylindrically focused at 102 mm (4 in.).

[b] Peak frequency 10 MHz, wideband, 6.4 mm (0.25 in.) active element diameter, flat lens.

[c] More gain needed than was available.

[d] Peak frequency 5 MHz, narrowband, 6.4 mm (0.25 in.) active element diameter, flat lens.

[e] Peak frequency 10 MHz, narrowband, 19 mm (0.75 in.) active element diameter, cylindrically focused lens at 102 mm (4 in.).

Table 1. (cont)

Transducer angle-of-incidence (deg)	Settings on S-80 Reflectoscope					
			Gain for 50% screen height of signal (db)			
			Adapter		Crack	
	Frequency (MHz)	Filter	For point 1	For point 2	For point 1	For point 2
18	5		20	20	3	17
		1	26	26	10	23
		2	28	29	12	27
		3	33	34	18	31
	WB		26	29	13	29
		1	32	34	19	35
		2	36	38	23	37
		3	40	42	29	43
19	5		16	19	3	17
		1	22	25	11	23
		2	25	29	13	26
		3	29	33	18	30
	WB		25	27	13	29
		1	30	33	20	35
		2	33	37	23	37
		3	38	40	29	42
20	5		18	22	19	19
		1	25	28	25	26
		2	28	32	28	29
		3	30	37	32	33
	WB		28	30	29	31
		1	33	36	34	37
		2	36	40	38	39
		3	41	44	42	45
			TRANSDUCER B[b]			
16	10		53	53	41	53
		1	62	62	49	62
		2	65	66	51	65
		3	67	69	59	70
	WB		51	55	37	51
		1	58	61	44	58
		2	62	63	49	63
		3	65	68	56	70

Table 1. (cont)

Transducer angle-of-incidence (deg)	Settings on S-80 Reflectoscope					
			Gain for 50% screen height of signal (db)			
			Adapter		Crack	
	Frequency (MHz)	Filter	For point 1	For point 2	For point 1	For point 2
17.3	10		50	49	36	43
		1	59	58	41	51
		2	61	60	48	56
		3	64	62	55	62
	WB		49	49	34	44
		1	56	57	42	51
		2	60	61	47	54
		3	63	65	55	61
18	10		54	50	38	45
		1	63	60	43	53
		2	65	62	48	58
		3	68	63	56	64
	WB		51	49	36	48
		1	59	57	46	54
		2	62	61	50	56
		3	65	64	57	62
19	10		55	50	39	55
		1	63	60	46	66
		2	66	62	49	68
		3	69	64	58	70
	WB		51	50	37	55
		1	58	57	44	62
		2	62	61	50	66
		3	67	65	58	(c)
20	10		57	50	53	52
		1	64	59	51	61
		2	67	62	54	66
		3	69	65	61	69
	WB		53	49	39	53
		1	60	57	45	61
		2	65	62	50	63
		3	67	66	59	65

Table 1. (cont)

Transducer angle-of-incidence (deg)	Settings on S-80 Reflectoscope					
			Gain for 50% screen height of signal (db)			
			Adapter		Crack	
	Frequency (MHz)	Filter	For point 1	For point 2	For point 1	For point 2
22	10		59	59	50	58
		1	67	67	59	66
		2	70	70	64	69
		3	(c)	(c)	68	(c)
	WB		56	57	53	59
		1	63	64	59	65
		2	69	70	64	(c)
		3	(c)	(c)	69	(c)
			TRANSDUCER C[d]			
16	5		41	42	26	38
		1	46	48	44	44
		2	49	51	46	48
		3	51	54	53	53
	WB		49	51	37	50
		1	55	57	32	56
		2	57	60	36	58
		3	60	64	41	65
17.3	5		37	39	24	32
		1	43	45	30	38
		2	46	49	33	40
		3	50	52	38	45
	WB		49	52	35	40
		1	53	56	41	46
		2	56	58	43	50
		3	60	61	50	57
18	5		39	40	25	40
		1	45	46	31	44
		2	48	49	34	48
		3	51	54	39	53
	WB		50	52	34	49
		1	55	58	41	54
		2	58	60	43	58
		3	61	63	50	63

Table 1. (cont)

Transducer angle-of-incidence (deg)	Settings on S-80 Reflectoscope					
			Gain for 50% screen height of signal (db)			
			Adapter		Crack	
	Frequency (MHz)	Filter	For point 1	For point 2	For point 1	For point 2
19	5		46	45	30	47
		1	52	52	36	52
		2	56	54	38	54
		3	59	59	44	59
	WB		55	54	38	54
		1	61	61	45	60
		2	65	63	49	64
		3	68	67	55	71
20	5		46	45	31	44
		1	52	51	37	50
		2	54	54	39	52
		3	57	59	44	57
	WB		53	53	39	57
		1	60	60	45	63
		2	62	64	48	66
		3	67	67	55	69
22	5		50	50	39	46
		1	54	55	44	51
		2	58	59	47	54
		3	63	62	51	58
	WB		60	58	48	57
		1	67	64	55	64
		2	70	68	57	66
		3	(c)	(c)	63	71
			TRANSDUCER D[e]			
16	10		48	48	33	44
	WB		54	55	40	50
17.3	10		48	47	33	45
	WB		53	52	39	50
18	10		47	47	33	43
	WB		52	52	40	50
19	10		48	49	35	44
	WB		54	53	41	52

Table 1. (cont)

Transducer angle-of-incidence (deg)	Settings on S-80 Reflectoscope					
			Gain for 50% screen height of signal (db)			
			Adapter		Crack	
	Frequency (MHz)	Filter	For point 1	For point 2	For point 1	For point 2
20	10		51	52	36	47
	WB		56	56	42	54
22	10		58	58	45	53
		1	68	66	53	61
		2	69	69	56	63
		3	(c)	71	61	68
	WB		62	62	51	62

Table 2. Performance of transducers

Transducer designation	Peak frequency (MHz)	Bandwidth	Active element diameter (mm)	Active element diameter (in.)	Flat lens	Cylindrically focused lens*	Peak clarity (db)	Peak clarity crack signal / adapter signal	Gain setting to detect crack at 50% height of screen (db)
A	5	narrow	19	0.75		X	17	7.1	3
B	10	wide	6.4	0.25	X		17	7.1	41
C	5	narrow	6.4	0.25	X		16	6.3	34
D	10	narrow	19	0.75		X	15	5.6	33

* 102 mm (4 in.)

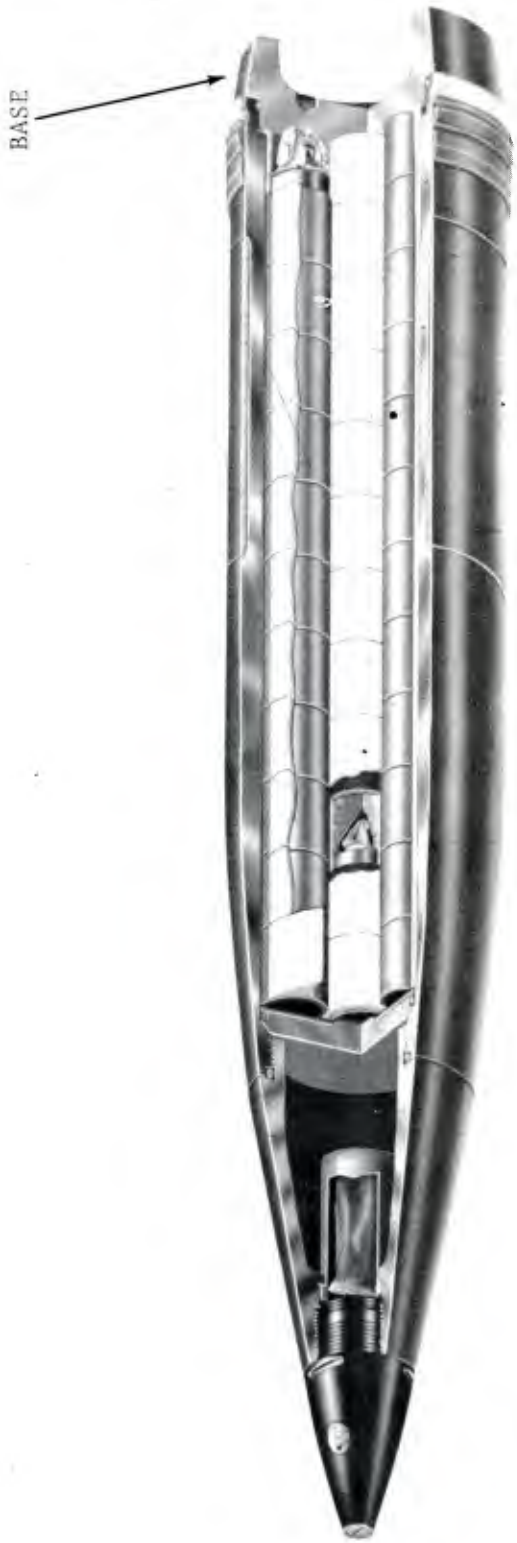

Figure 1. 155-mm M483A1 projectile

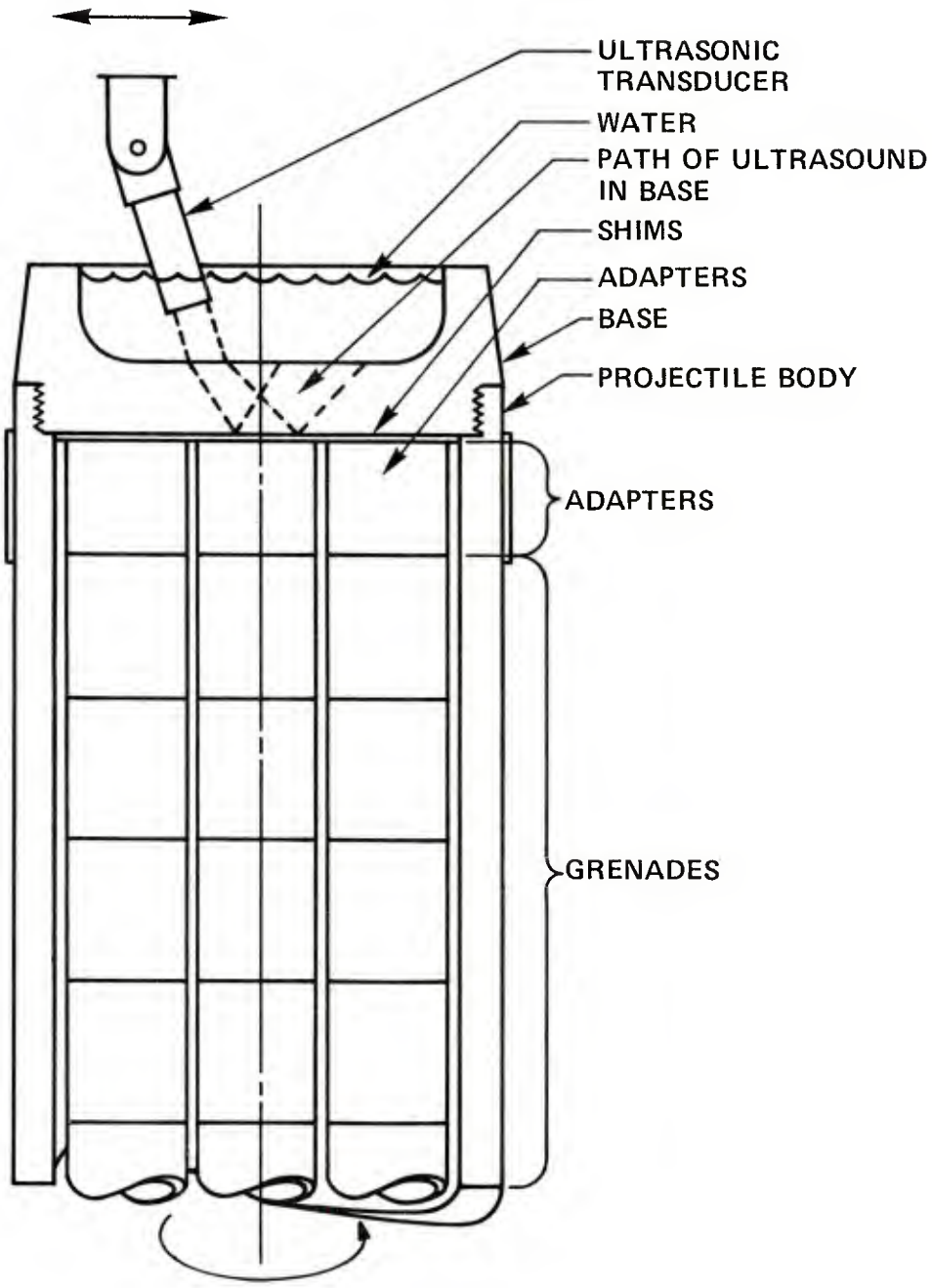

Figure 2. Ultrasonic inspection setup for a cracked base

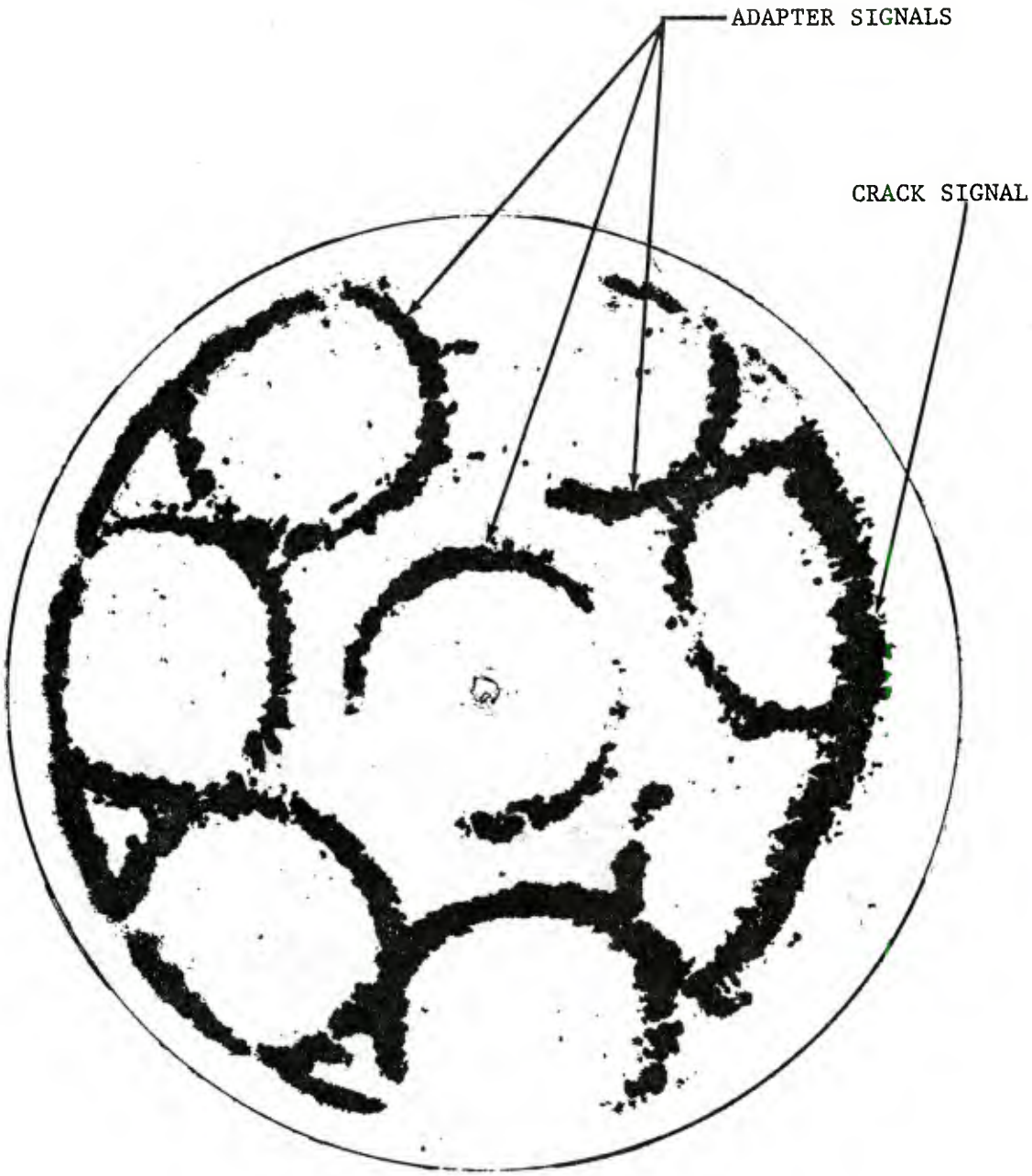

Figure 3. Ultrasonic C-scan showing distribution of crack and adapter signals

Figure 4. Simulated projectile body

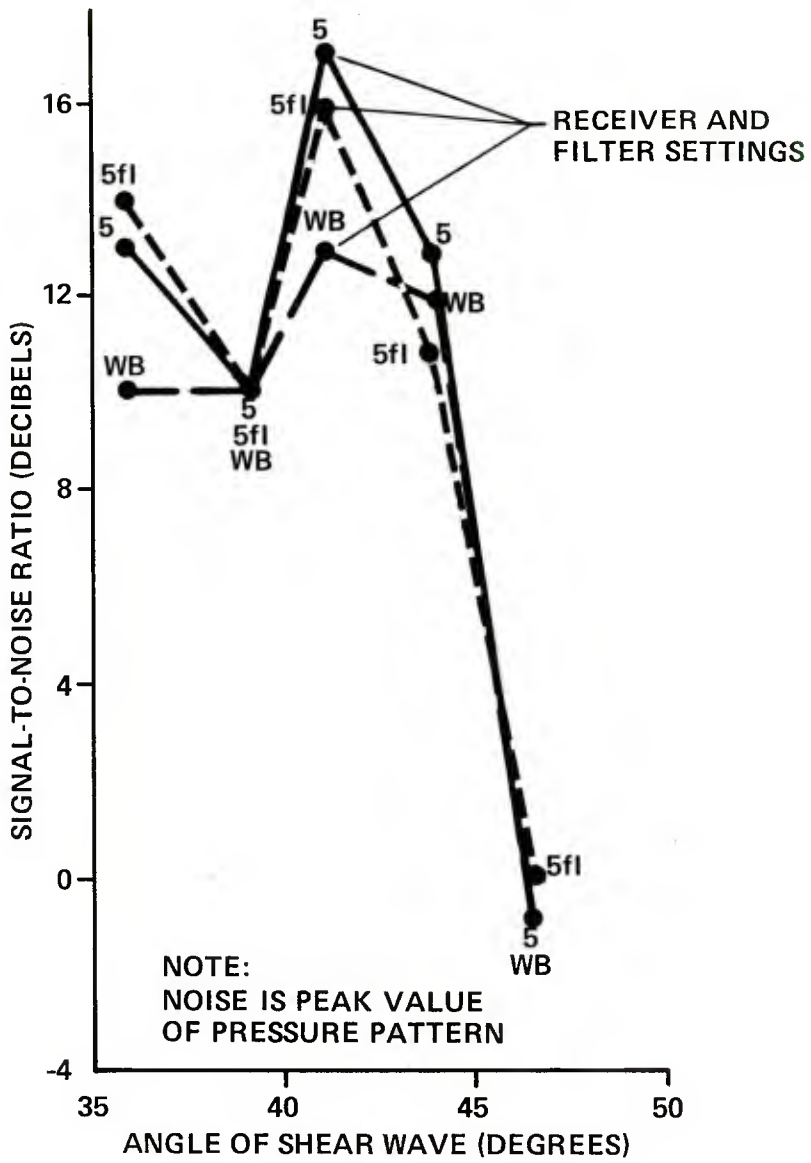

Figure 5. Clarity of ultrasonic echoes from a natural crack by use of transducer A (5 MHz, narrowband, 19-mm diameter active element, cylindrically focused at 102 mm)

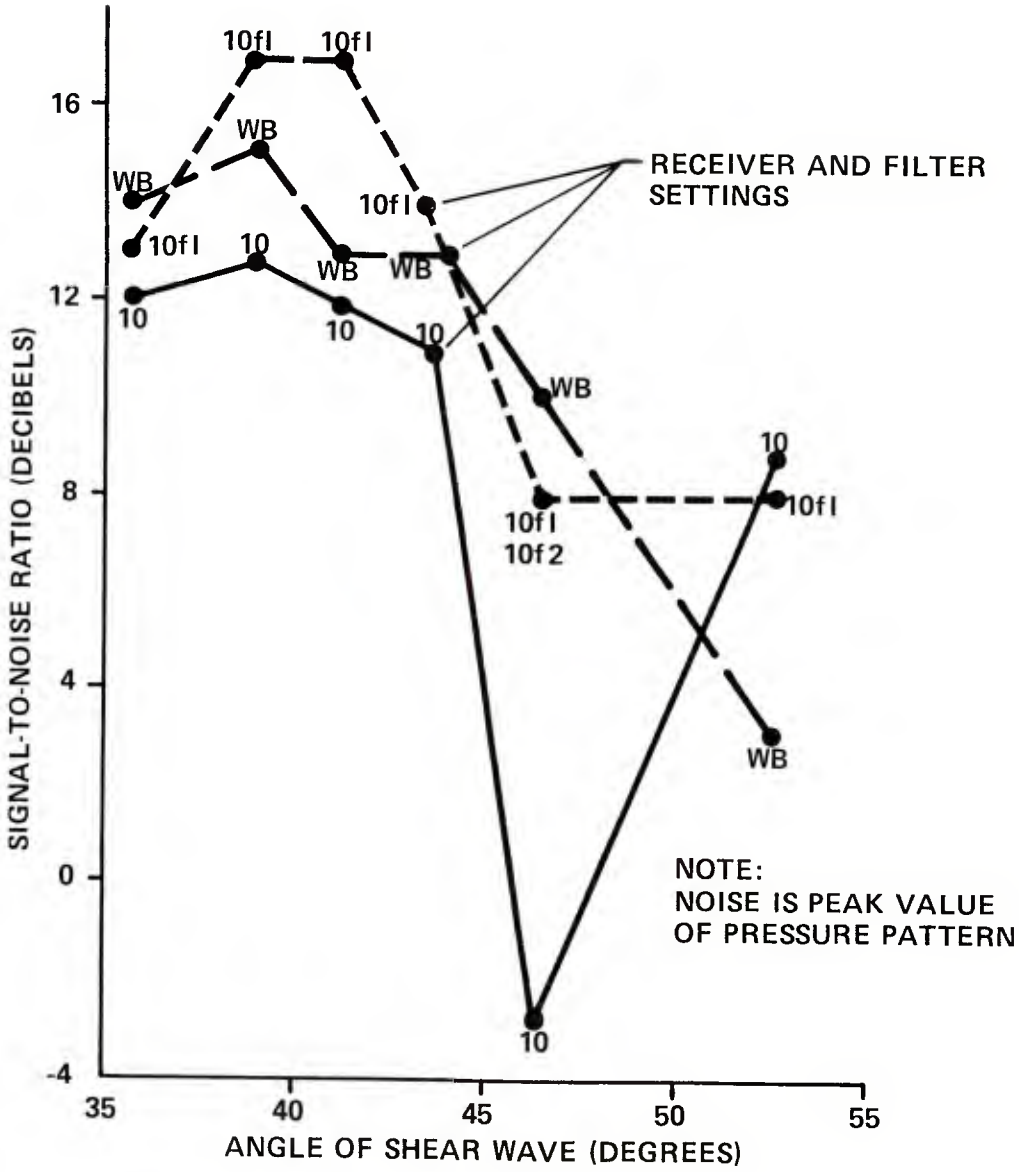

Figure 6. Clarity of ultrasonic echoes from a natural crack by use of transducer B (10 MHz, wideband, 6.4-mm diameter active element, flat lens)

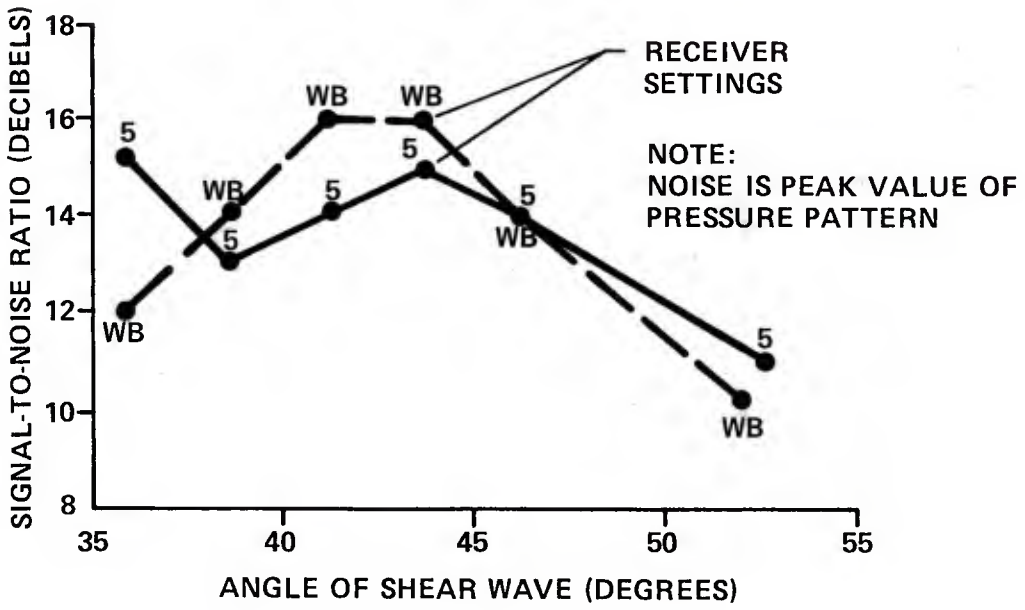

Figure 7. Clarity of ultrasonic echoes from a natural crack by use of transducer C (5 MHz, narrowband, 6.4 mm diameter active element, flat lens)

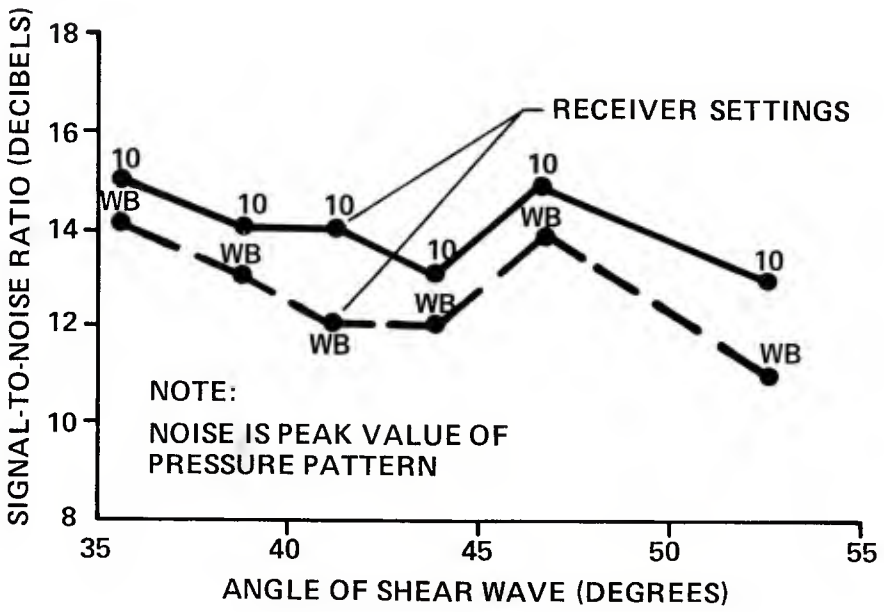

Figure 8. Clarity of ultrasonic echoes from a natural crack by use of transducer D (10 MHz, narrowband, 19 mm diameter active element, cylindrically focused at 102 mm)

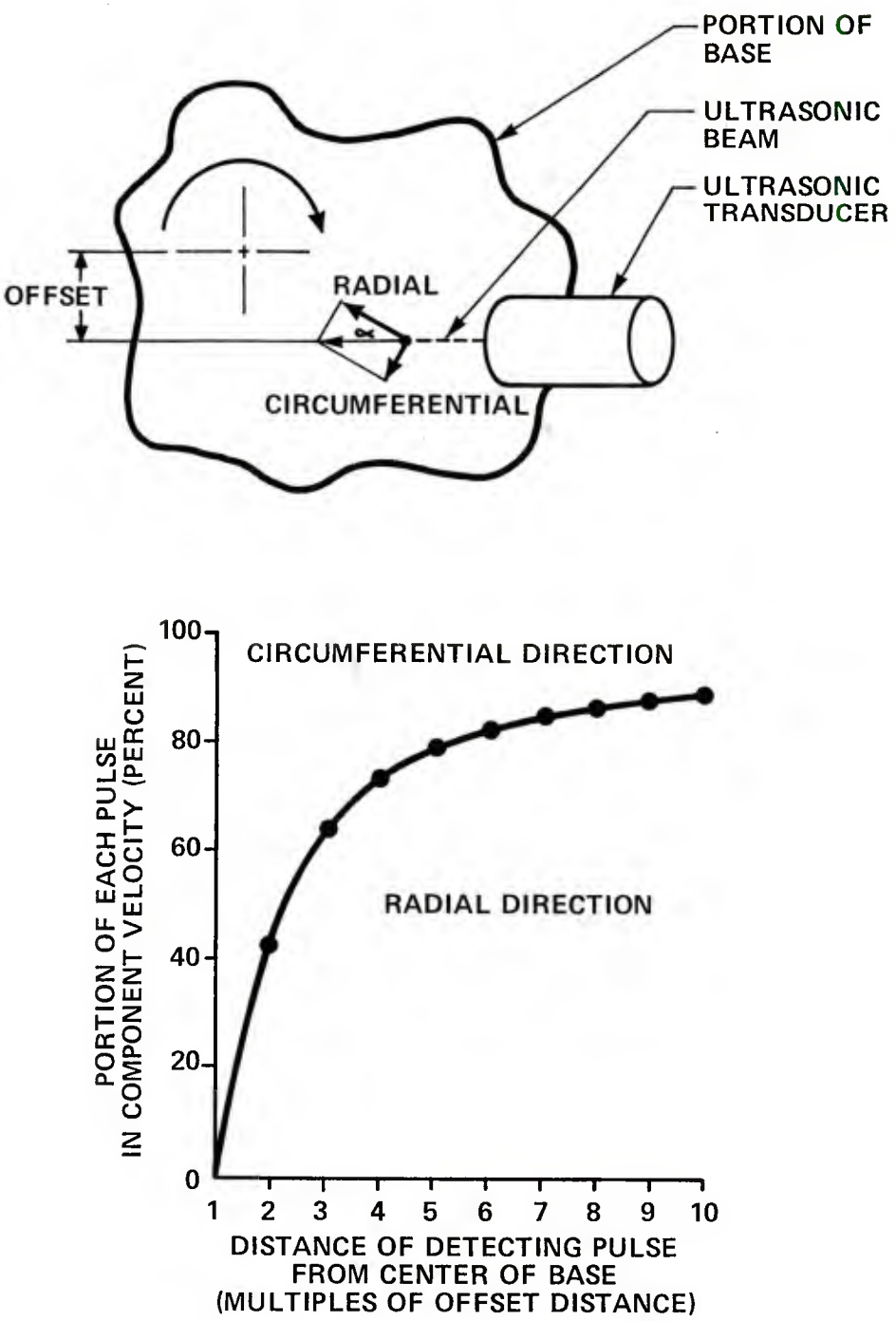

Figure 9. Relationship of radial and circumferential component velocities of an offset ultrasonic beam

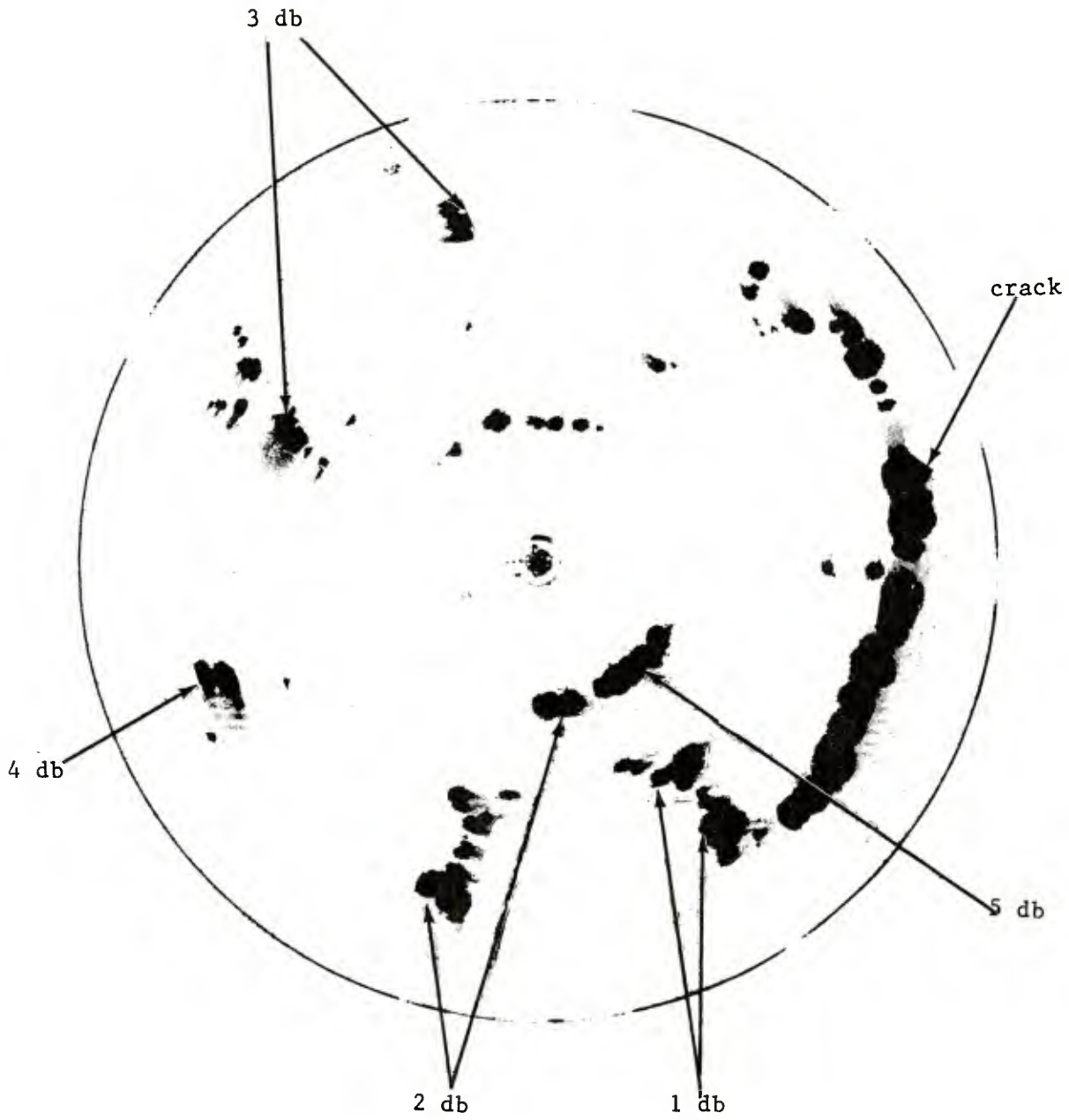

Figure 10. Ultrasonic C-scan showing peak signals from a cracked base mounted in the simulated projectile body by use of a transducer B offset 0.5 mm to the right

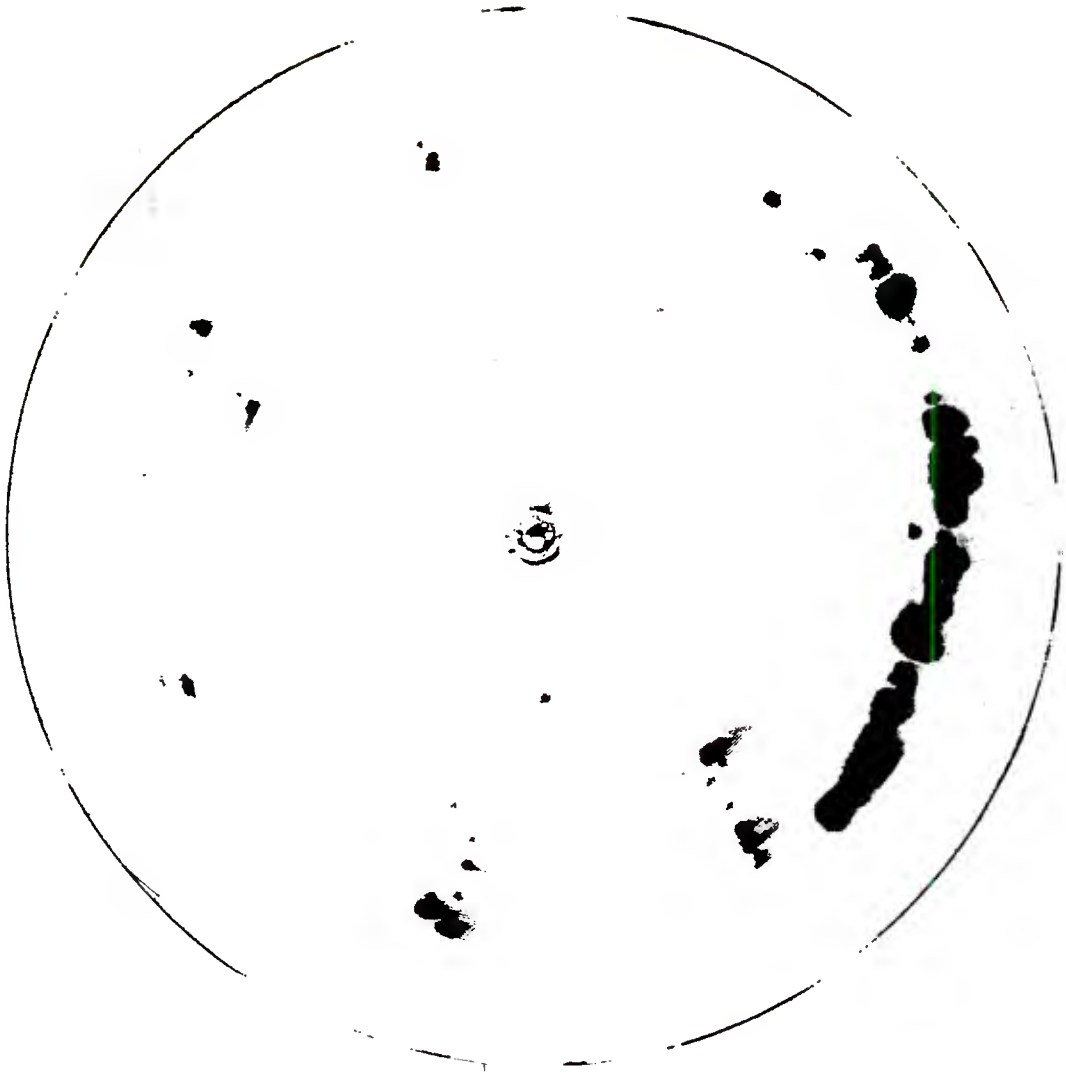

Figure 11. Ultrasonic C-scan of cracked base mounted in the simulated projectile body by use of transducer B offset 1.5 mm to the right

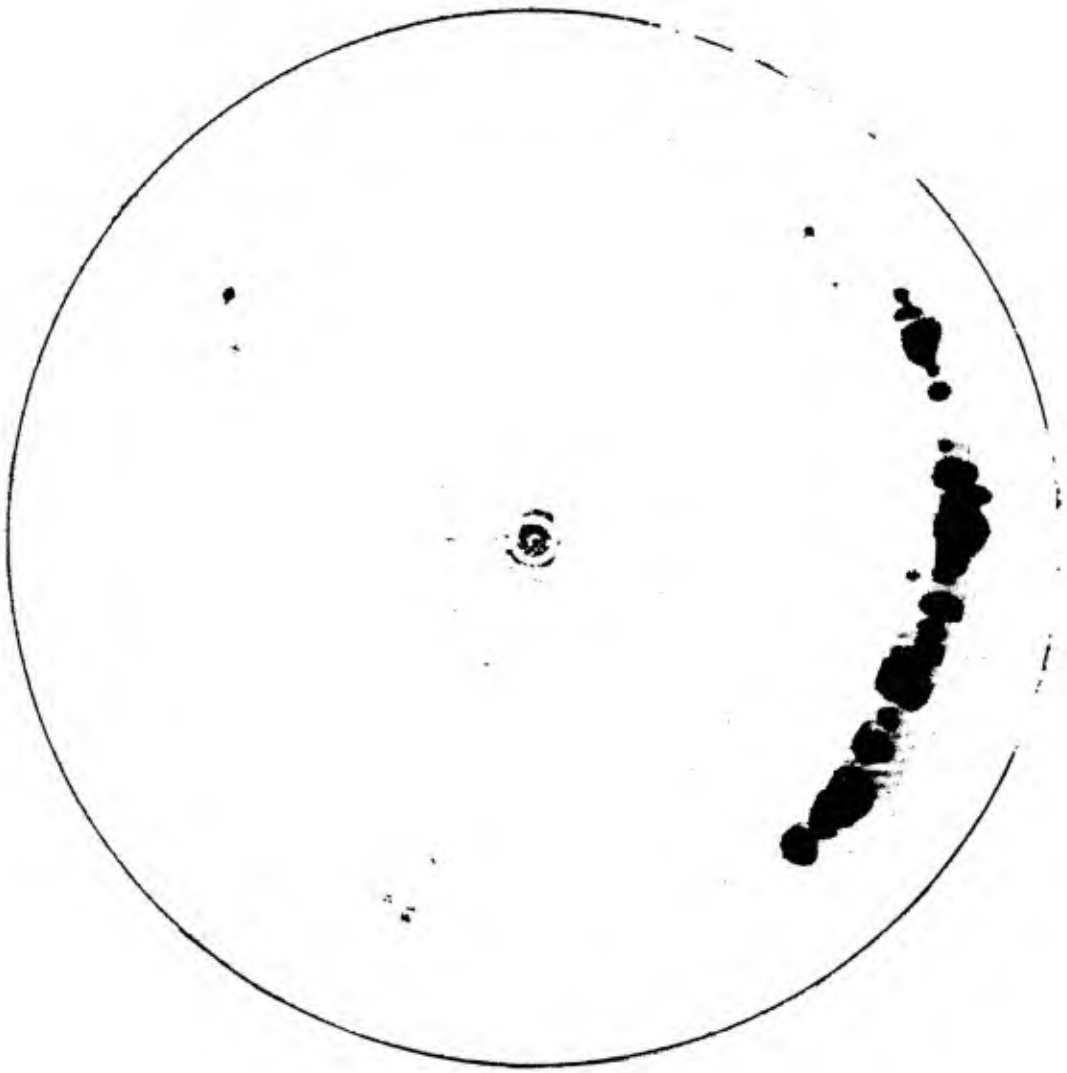

Figure 12. Ultrasonic C-scan of cracked base mounted in the simulated projectile body by use of transducer B offset 2.5 mm to the right

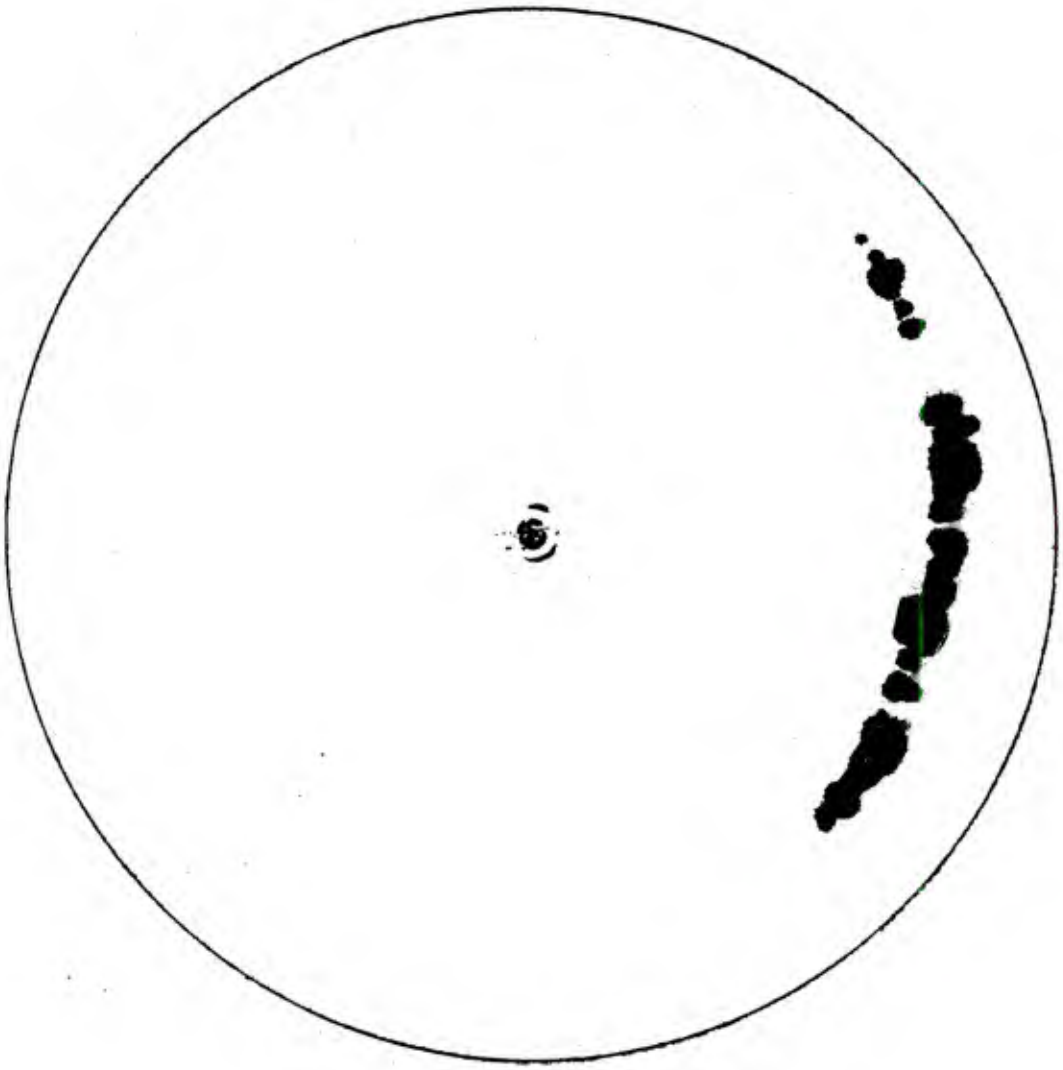

Figure 13. Ultrasonic C-scan of cracked base mounted in the simulated projectile body by use of transducer B offset 3.5 mm to the right

Figure 14. Ultrasonic C-scan of cracked base mounted in the simulated projectile body by use of transducer B offset 4.5 mm to the right

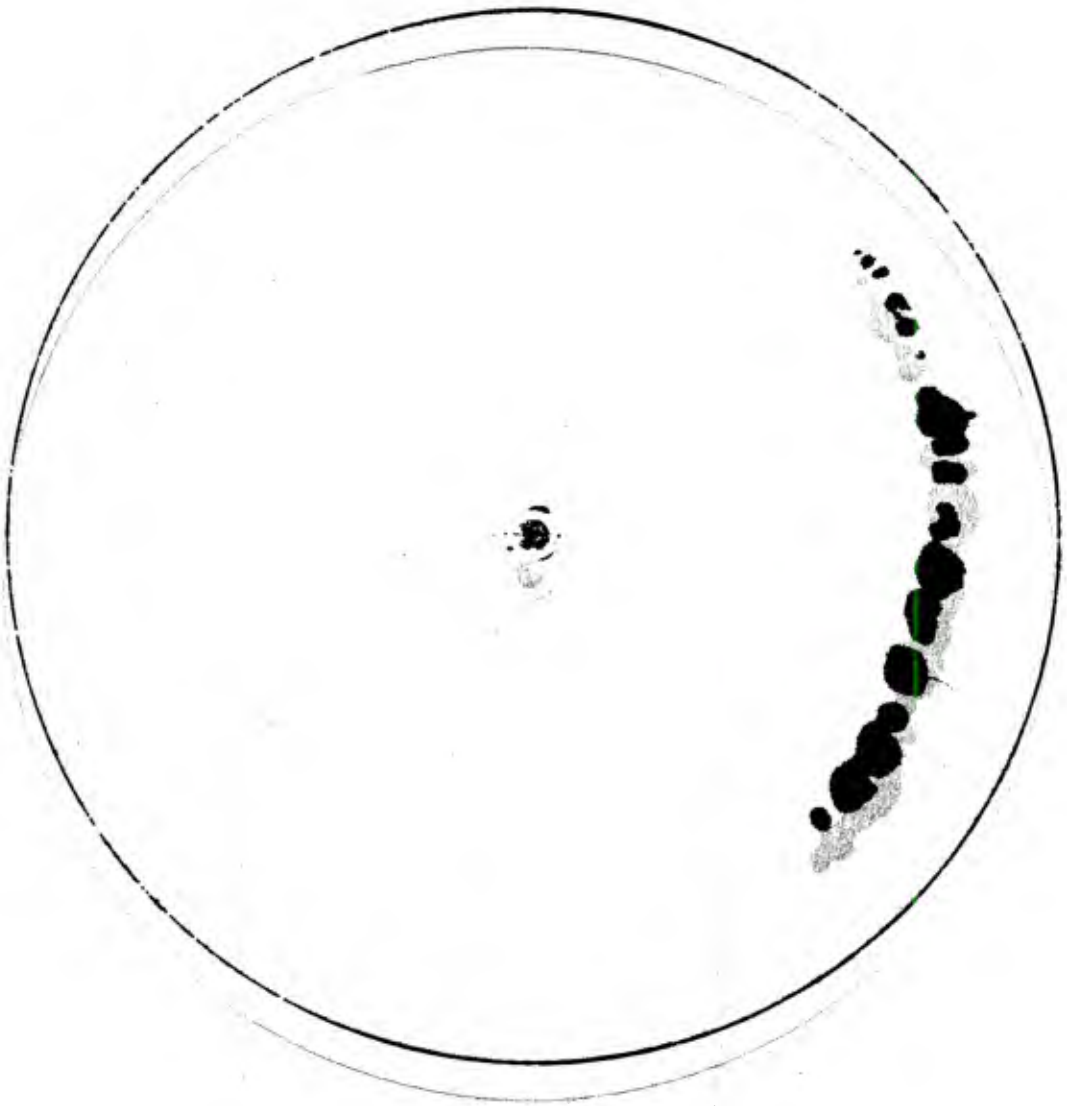

Figure 13. Ultrasonic C-scan of cracked base mounted in the simulated projectile body by use of transducer B offset 5.5 mm to the right

Figure 15. Ultrasonic C-scan of cracked base mounted in the simulated projectile body by use of transducer B offset 5.5 mm to the right

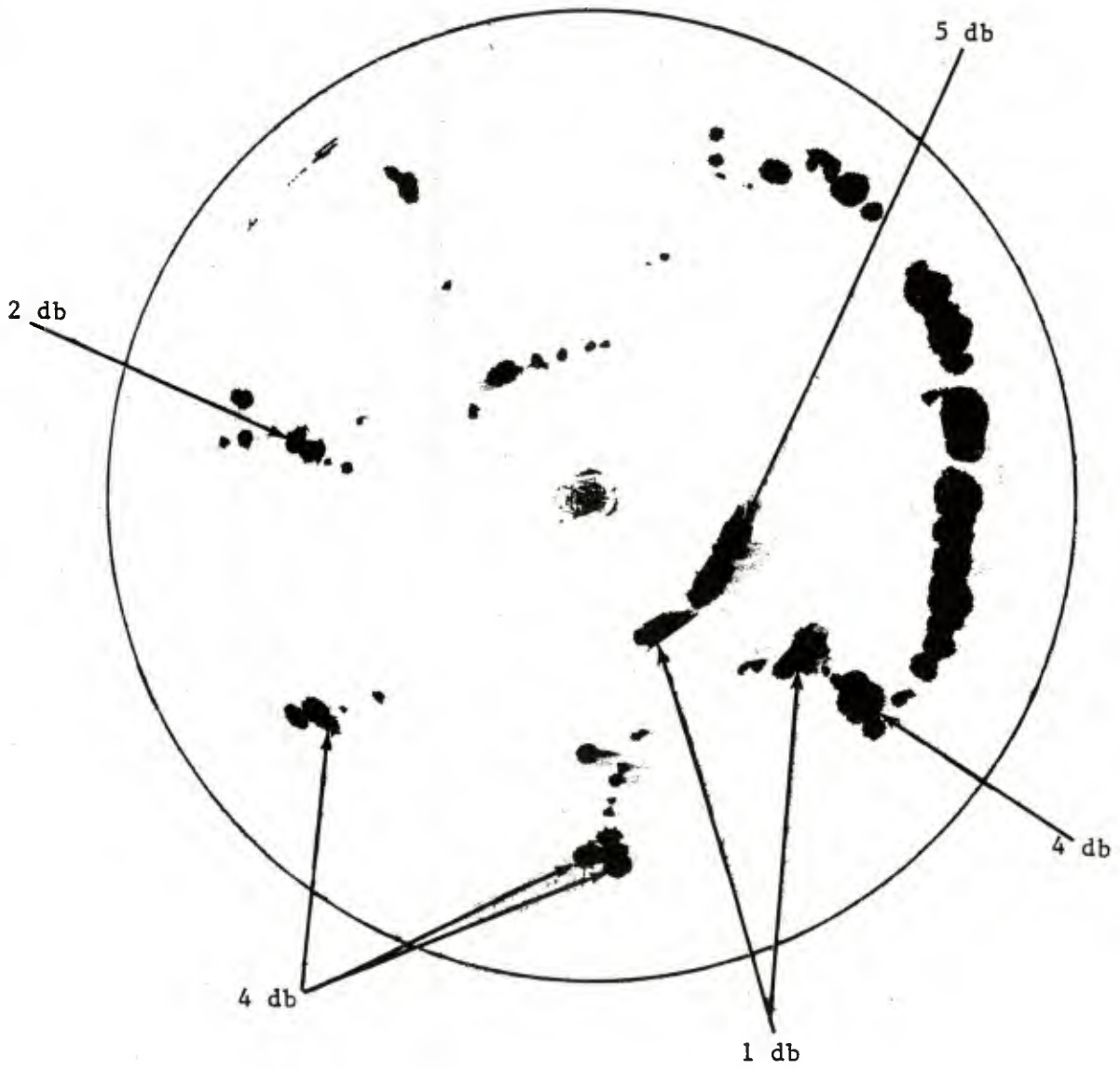

Figure 16. Ultrasonic C-scan showing peak signals from a cracked base mounted in the simulated projectile body by use of transducer B offset 0.5 mm to the left

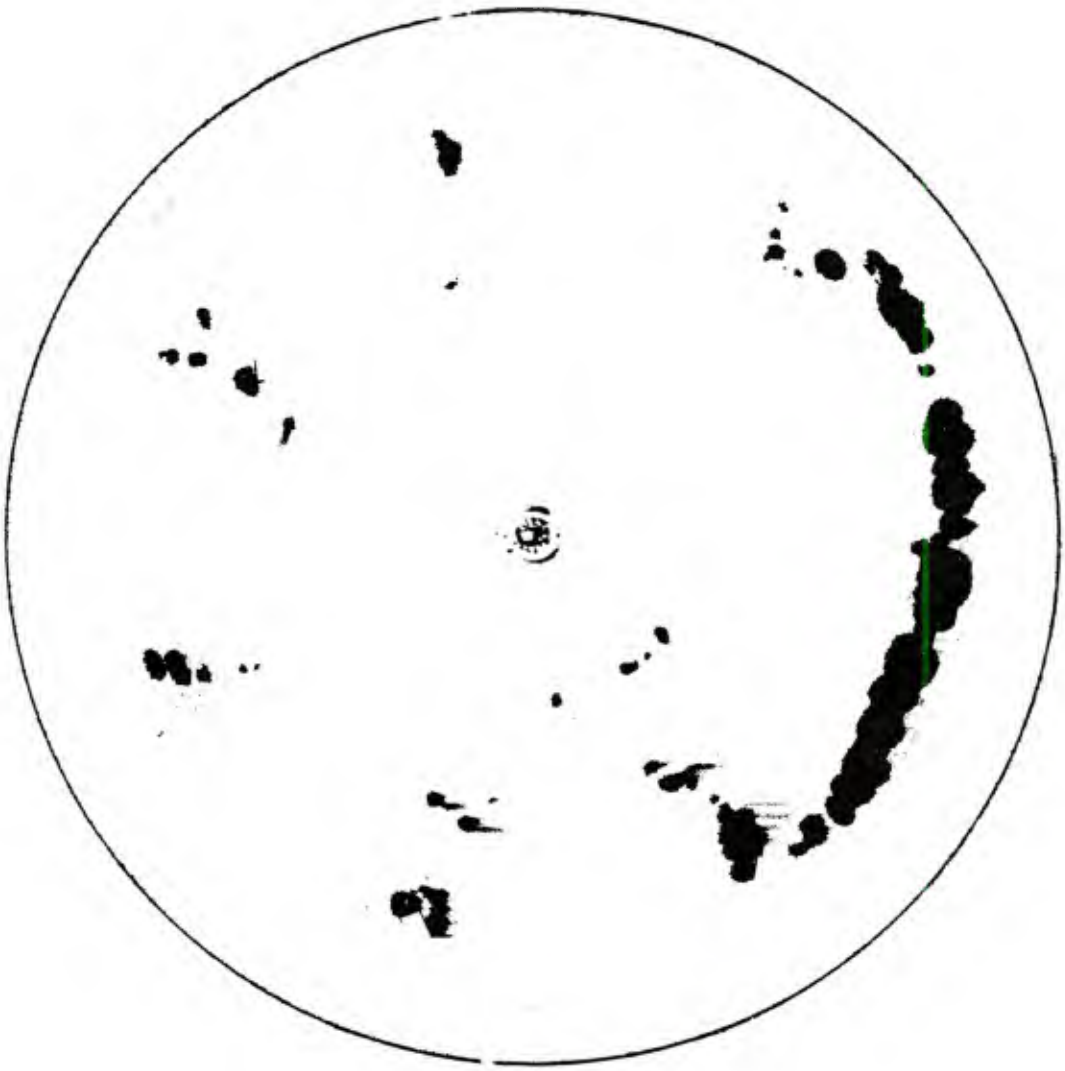

Figure 17. Ultrasonic C-scan of cracked base mounted in the simulated projectile body by use of transducer B offset 1.5 mm to the left

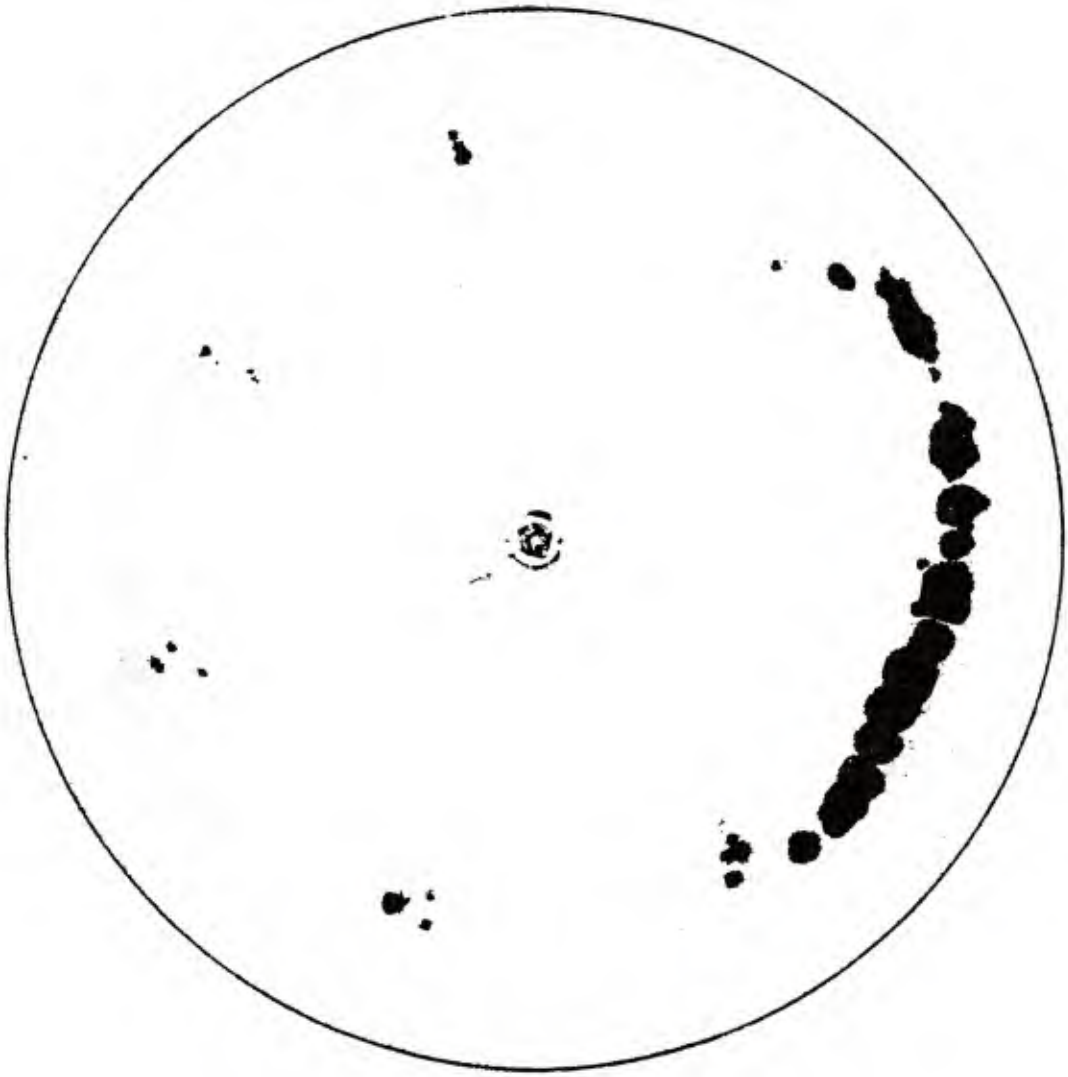

Figure 18. Ultrasonic C-scan of cracked base mounted in the simulated projectile body by use of transducer B offset 2.5 mm to the left

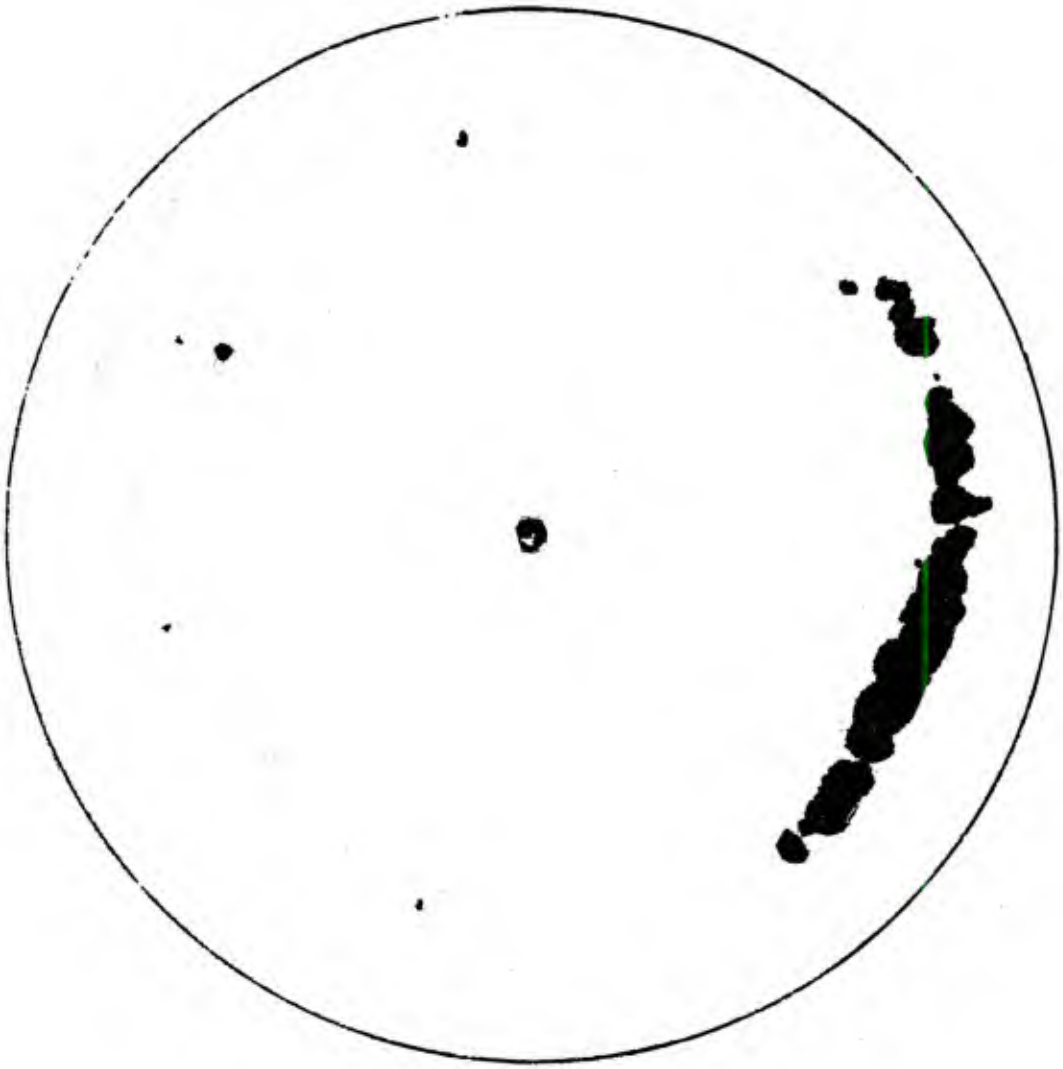

Figure 19. Ultrasonic C-scan of cracked base mounted in the simulated projectile body by use of transducer B offset 3.5 mm to the left

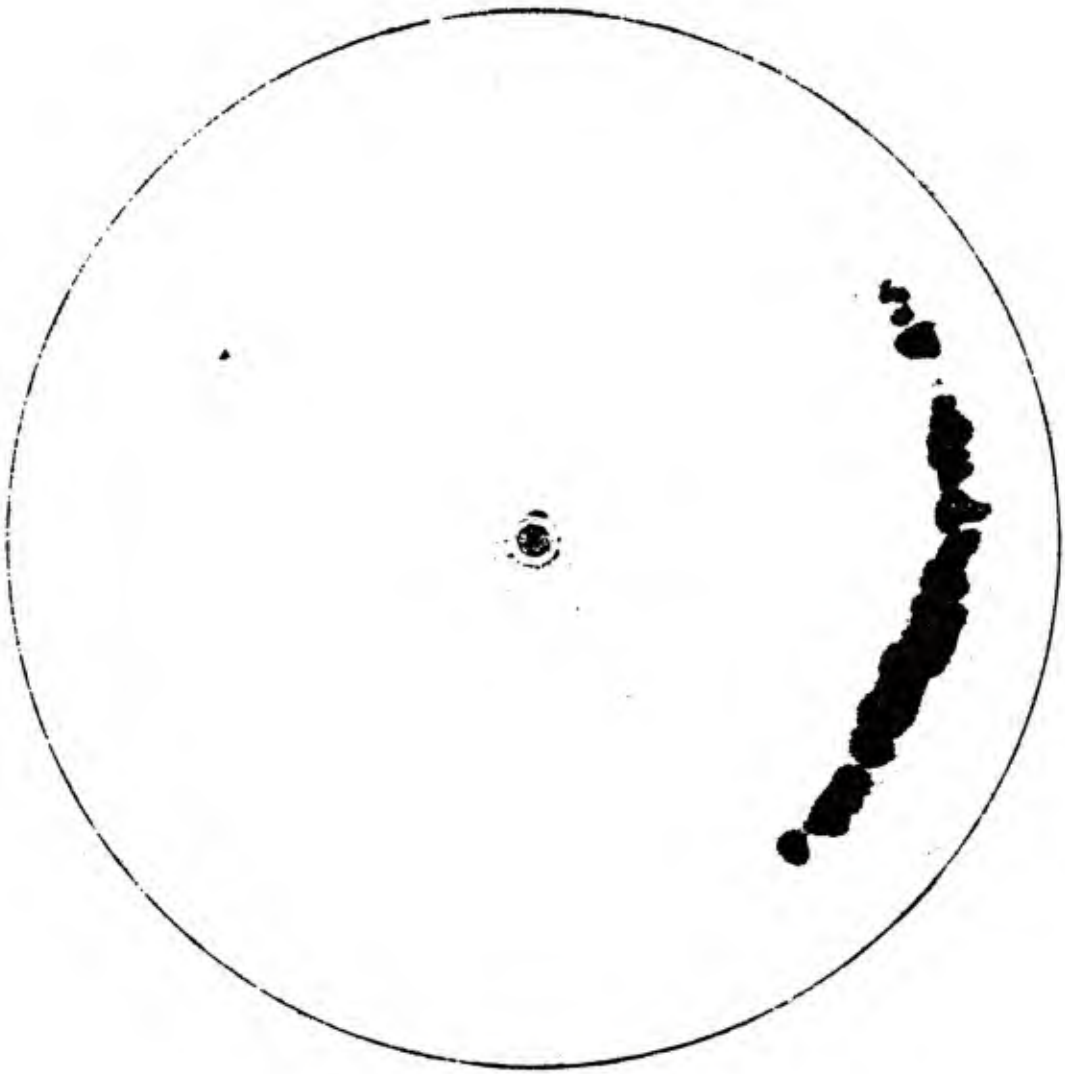

Figure 20. Ultrasonic C-scan of cracked base mounted in the simulated projectile body by use of transducer B offset 4.5 mm to the left

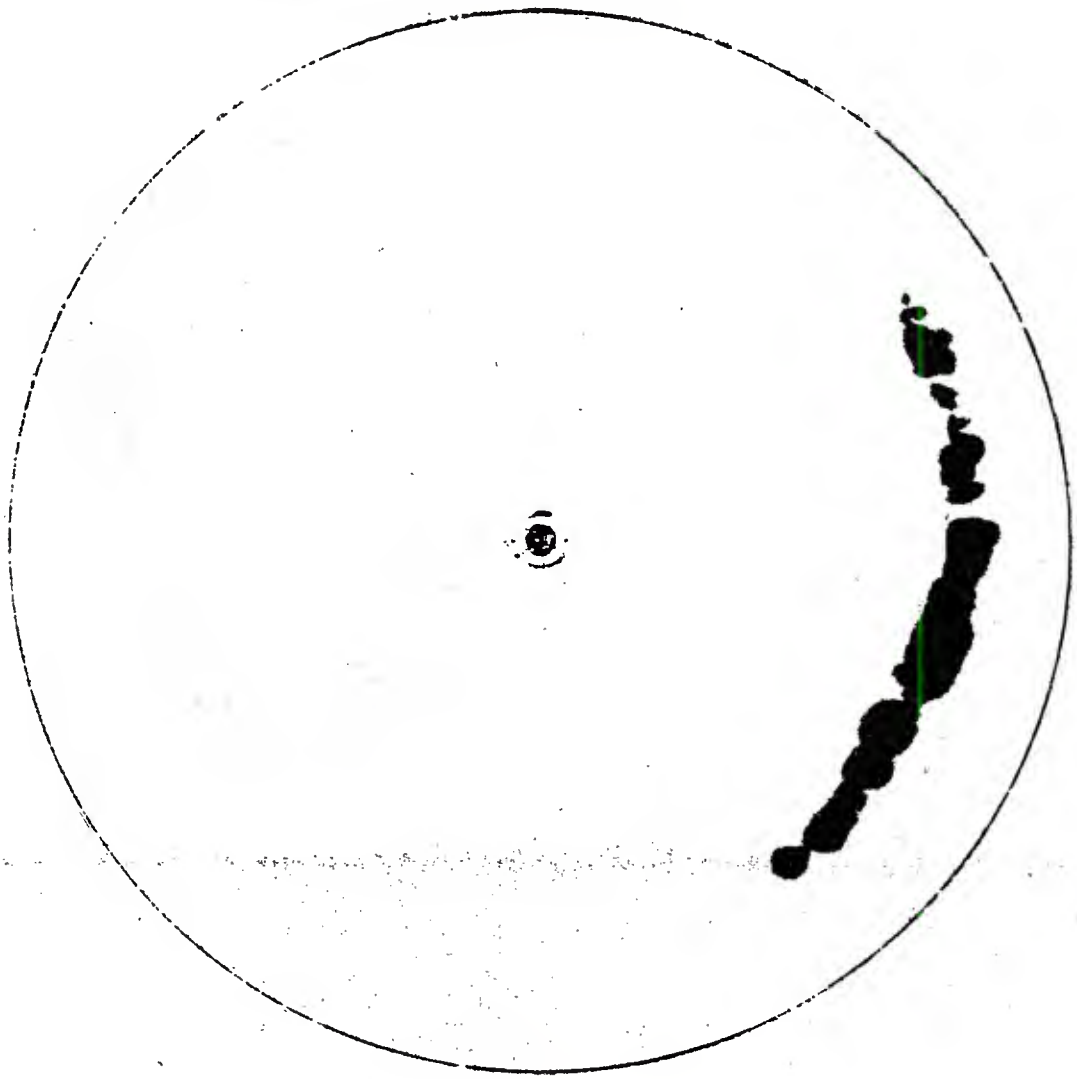

Figure 21. Ultrasonic C-scan of cracked base mounted in the simulated projectile body by use of transducer B offset 5.5 mm to the left

Figure 22. Simulated ultrasonic C-scan of cracked base mounted in the simulated projectile body by use of two transducers B spaced 1 mm apart and aimed at the same spot

Figure 23. Simulated ultrasonic C-scan of cracked base mounted in the simulated projectile body by use of two transducers B spaced 3 mm apart and aimed at the same spot

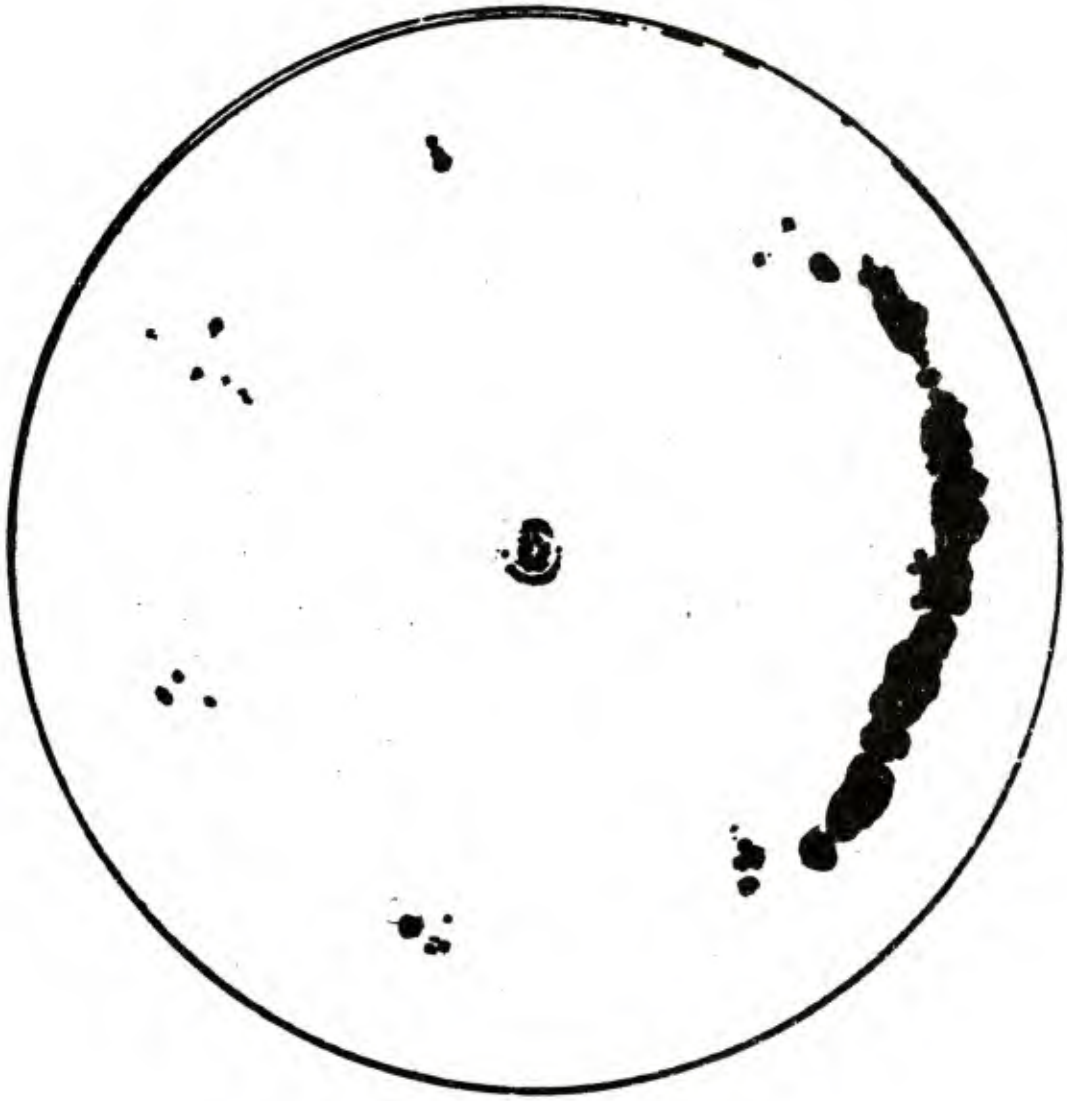

Figure 24. Simulated ultrasonic C-scan of cracked base mounted in the simulated projectile body by use of two transducers B spaced 5 mm apart and aimed at the same spot

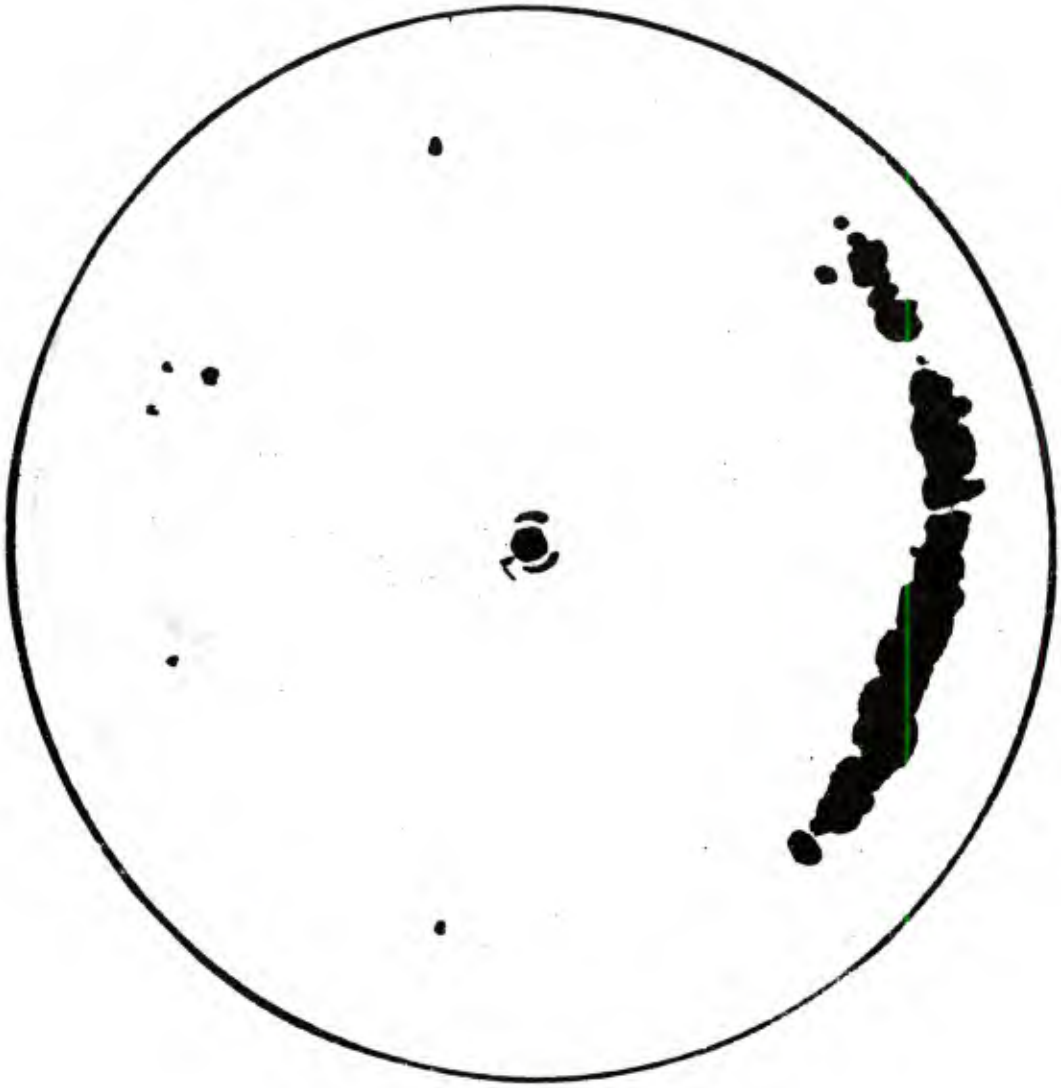

Figure 25. Simulated ultrasonic C-scan of cracked base mounted in the simulated projectile body by use of two transducers B spaced 7 mm apart and aimed at the same spot

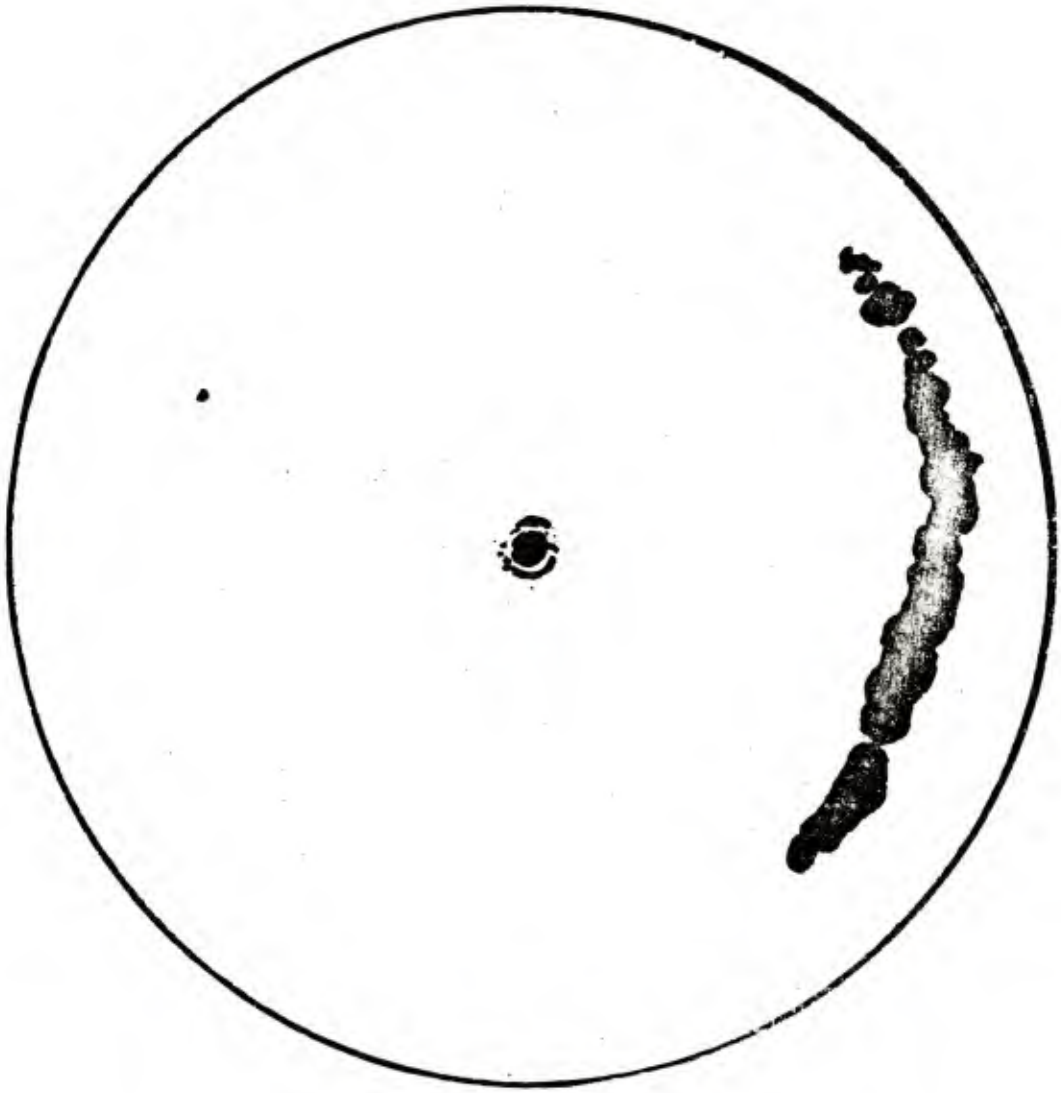

Figure 26. Simulated ultrasonic C-scan of cracked base mounted in the simulated projectile body by use of two transducers B spaced 9 mm apart and aimed at the same spot

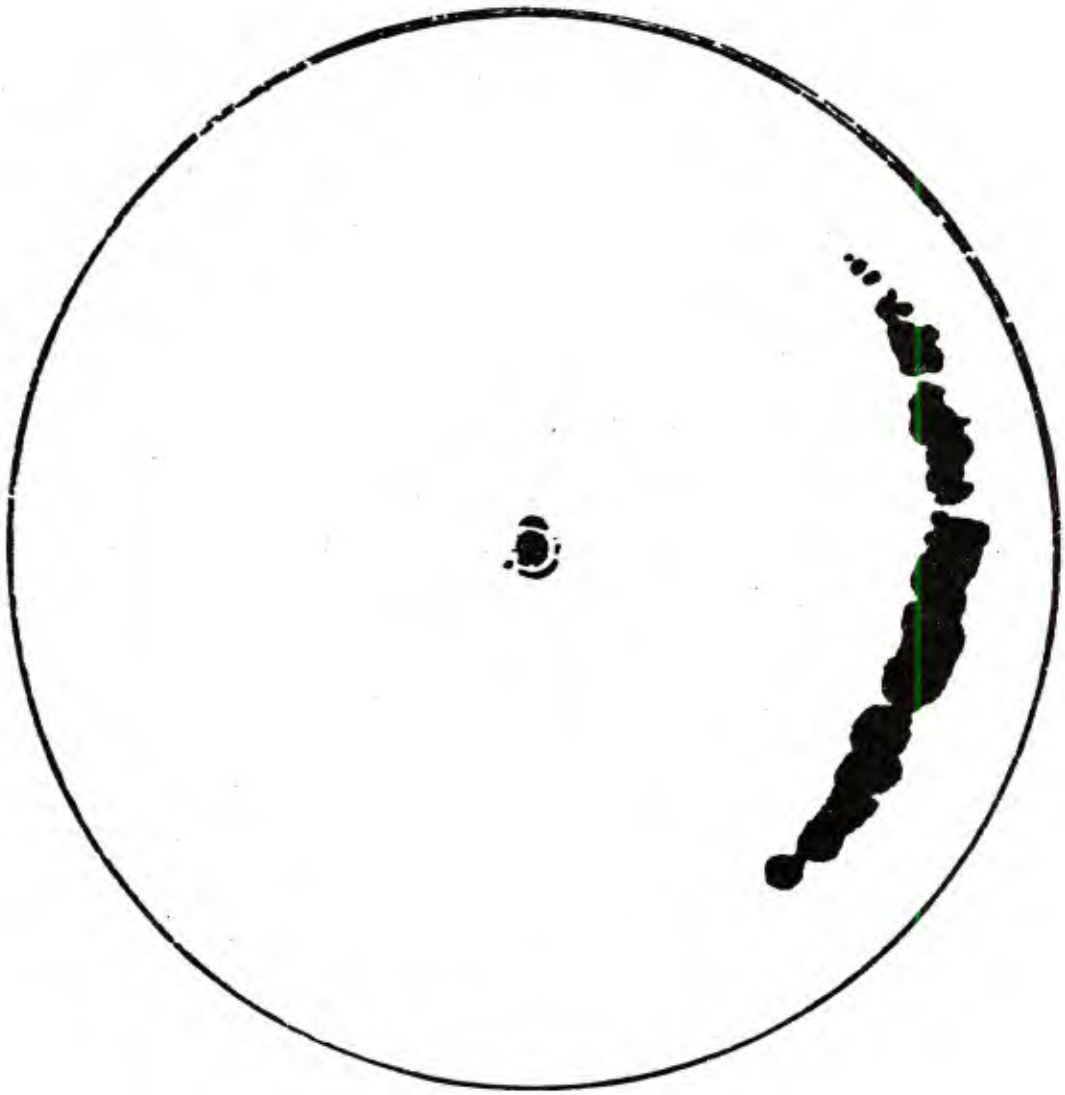

Figure 27. Simulated ultrasonic C-scan of cracked base mounted in the simulated projectile body by use of two transducers B spaced 11 mm apart and aimed at the same spot

DISTRIBUTION LIST

Commander
U.S. Army Armament Research
and Development Command
ATTN: DRDAR-QA
DRDAR-QAS
DRDAR-QAA
DRDAR-QAF
DRDAR-QAC
DRDAR-QAR
DRDAR-QAN
DRDAR-QAM
DRDAR-LCA
DRDAR-LCE
DRDAR-LCM
DRDAR-LCW
DRDAR-LCN
DRDAR-SCP
DRDAR-SCA
DRDAR-SCS
DRDAR-SCM
DRDAR-TSE
DRDAR-TSB
DRDAR-TSS (5)
DRDAR-TD
DRDAR-TDS
DRDAR-TDA
DRDAR-TDC
DRDAR-GCL
Dover, NJ 07801

Project Manager
Cannon Artillery Weapons Systems
ATTN: DRCPM-CAWS
Dover, NJ 07801

Project Manager
Division Air Defense (DIVAD) Gun
ATTN: DRCPM-ADG
Dover, NJ 07801

Commander
U.S. Army Munitions Production
Base Modernization Agency
ATTN: SARPM-PBM
Dover, NJ 07801

Product Manager for
30mm Ammunition
ATTN: DRCPM-AAH-30MM
Dover, NJ 07801

Project Manager
Tank Main Armament Systems
ATTN: DRCPM-TMA
Dover, NJ 07801

Commander
Aberdeen Proving Ground
ATTN: STEAP-MT-T, B. 525
Aberdeen Proving Ground, MD 21005

Commander, Code 33
Naval Weapons Station
ATTN: Engineering and Science Div,
Weapon Quality Engineering Center
Concord, CA 94520

Commander
Dahlgren Navy Weapons Laboratory
ATTN: G53 (Material Science Branch)
Dahlgren, VA 22448

Director
U.S. Army Defense Ammunition
Center and School
ATTN: SARWR-QA
Watervliet, NY 12189

Commander
Foreign Science and Technical Center
1220 Seventh Street, NE
ATTN: DRXST-IS3
Charlottesville, VA 22901

Commander
Hawthorne Army Ammunition Plant
DZB Box A
ATTN: Technical Services
Babbitt, NV 89416

Commander
Indiana Army Ammunition Plant
ATTN: SARIN-QA
Charlestown, IN 47111

Commander
U.S. Navy Ordnance Station
ATTN: Code 40
Indian Head, MD 20640

Commander
Iowa Army Ammunition Plant
ATTN: SARIO-QA
Middletown, IO 52638

Commander
Jefferson Proving Ground
ATTN: STEJP-MTD
Madison, IN 47250

Commander
U.S. Army White Sands Missile Range
ATTN: STEWS-QA-E, B124
White Sands, NM 88002

Commander
Kansas Army Ammunition Plant
ATTN: SARKA-QA
Parsons, KS 67357

Commander
Lake City Army Ammunition Plant
ATTN: SARLC-QA
E. Independence, MO 64050

Commander
Lone Star Army Ammunition Plant
ATTN: SARLS-QA
Texarkana, TX 75501

Commander
Longhorn Army Ammunition Plant
ATTN: SARLO-QA
Marshall, TX 75670

Commander
Louisiana Army Ammunition Plant
ATTN: SARLA-QA
Shreveport, LA 71130

Commander
McAlester Army Ammunition Plant
ATTN: SARMC-QA
McAlester, OK 74501

Commander
Milan Army Ammunition Plant
ATTN: SARMI-QA
Milan, TN 38358

Commander
U.S. Navy Research Laboratory
4555 Overlook Avenue
ATTN: Code 5835
Washington, DC 20375

Commander
U.S. Navy Weapons Center
ATTN: Code 3682
China Lake, CA 93555

Commander
u.S. Navy Weapons Station
ATTN: Code 40
Charleston, SC 29408

Commander
U.S. Navy Weapons Station
ATTN: Code 401
Colts Neck, NJ 07722

Commander
U.S. Navy Weapons Station
ATTN: Code F321
Fallbrook, CA 92028

Commander
U.S. Navy Weapons Station
ATTN: Code 40
Yorktown, VA 23691

Commander
U.S. Navy Weapons Support Center
ATTN: Code 40
Crane, IN 47522

Commander
U.S. Army Pine Bluff Arsenal
ATTN: SARPB-QA
Pine Bluff, AR 71602

Commander
Red River Army Ammunition Plant
ATTN: SARRR-QA
Texarkana, TX 75501

Commander
U.S. Army Armament Materiel
Readiness Command
ATTN: DRSAR-LE
DRSAR-LEM-M
DRSAR-LEP-L
DRSAR-QA
Rock Island, IL 61299

Administrator
Defense Technical Information Center
ATTN: Accessions Division (12)
Cameron Station
Alexandria, VA 22314

Director
U.S. Army Materiel Systems
Analysis Activity
ATTN: DRXSY-MP
Aberdeen Proving Ground, MD 21005

Commander/Director
Chemical Systems Laboratory
U.S. Army Armament Research
and Development Command
ATTN: DRDAR-CLB-PA
DRDAR-CLJ-L
DRDAR-CLN
APG, Edgewood Area, MD 21010

Director
Ballistics Research Laboratory
U.S. Army Armament Research
and Development Command
ATTN: DRDAR-TSB-S
DRDAR-BLB
DRDAR-BLI
DRDAR-BLL
Aberdeen Proving Ground, MD 21005

Chief
Benet Weapons Laboratory, LCWSL
U.S. Army Armament Research
and Development Command
ATTN: DRDAR-LCB-TL
Watervliet, NY 12189

Director
U.S. Army TRADOC Systems
Analysis Activity
ATTN: ATAA-SL
White Sands Missile Range, NM 88002

Commander
U.S. Army Research and
Technology Laboratories
ATTN: DAVDL-EU
Ft. Eustis, VA 23604

Director
U.S. Army Research and
Technology Laboratories
AMES Research Center
ATTN: DAVDL-AS
Moffett Field, CA 94035

Director
U.S. Defense Ammunition Center and School
ATTN: SARAC-DEN
Savanna, IL 61074